Coupled Enzymatic Oxidation of Methanol

by

David Harrison
B.Sc., M.Sc., University of Victoria, 2002

A Thesis Submitted in Partial Fulfillment of the
Requirements for the Degree of

Master of Science
in the Department of Biology

Abstract

The enzymatic oxidation of methanol was explored to evaluate the efficacy of coupled enzyme hydrogen production. The "domain A" motif, responsible for tight NAD- binding of the *Bacillus methanolicus* C1 methanol dehydrogenase (BmMDH), was mutated by the introduction of a serine to glycine amino acid (aa) substitution at position 97 aa to permit methanol oxidation without the presence of an activator protein from the same organism. The *Wautersia eutropha* H16 soluble NAD^+-dependent [NiFe]-hydrogenase (SH) was expressed by culturing the bacterium under aerobic carbon-limiting conditions. Both the BmMDH and the SH were partially purified. The oxidation of methanol by MDH and hydrogen by SH were assayed, respectively. The BmMDH and the SH were permitted to co-react in the presence of methanol, NAD, and the low potential redox dye benzyl viologen (BV). The reaction conditions resulted in the reduction of BV, indicating that a flow of electrons originating from the oxidation of methanol by BmMDH to the redox dye via the SH had occurred. Our results suggest hydrogen can be produced from the oxidation of methanol using the couple enzyme strategy.

Supervisor: Dr. David Levin, (Biology)

Table of Contents

Acknowledgments

Firstly, I would like to thank my supervisor, Dr. Levin, for giving me the opportunity and support to explore my intellectual curiosities. I would also like to thank my committee members, Dr. Hintz and Dr. von Aderkas, for their time and patience. The appreciation is further extended to Dr. von Aderkas and Dr. Anholt for their help and words of encouragement over the waning hours of my degree.

I would also like to thank the members of the Levin Lab I had the pleasure to work with, for without their help and friendship my experience would have been quite "ordinary." It is with a heavy heart that I say goodbye. Thank you, Simon, Tina, Beatrix, John, Roberto, Elisa, Kit, Julia, Jen, Stacy, Dan and Carlo.

To Gord Cooney and Simon Duffy, thank you for "taking me in" during my greatest time of need. Your kindness will not be forgotten.

Finally, to my family, without you I would not have had the strength or courage to follow my dreams. I love you Mom, Dad, Sarah, Mason, Paige, Genny and Russ.

I am done...(for now)...

List of Figures

List of Tables

List of Abbreviations

ADH	Alcohol dehydrogenase
BmMDH	*Bacillus methanolicus* C1 methanol dehydrogenase
BV	Benzyl viologen
BSA	Bovine serum albumin
CTAB	N-cetyltrimethylammonium bromide
DSMO	Dimethyl sulfoxide
DTT	Dithiothreitol
FAD	Flavin adenine dinucleotide
Fe-S	Iron sulfur cluster
FGN	Mineral media supplemented with 0.2 % (wt/vol) fructose and 0.2 % (vol/vol)
FMN	Flavin adenine mononucleotide
FN	Mineral media supplemented with 0.4 % (wt/vol) fructose
GDH	Glucose dehydrogenase
H_2ase	Hydrogenase
HPS	3-hexulose-6-phosphate synthase
kDa	Kilodalton
K_m	Michaelis constant
LB amp$^+$	Luria-Bertani plus ampicillin
MBH	*Wautersia eutropha* membrane-bound H_2ase
MDH	Methanol dehydrogenase enzyme
M_r	Relative molecular mass
NAD$^+$	Oxidized nicotinamide adenine dinucleotide
NADH	Reduced nicotinamide adenine dinucleotide
NADP(H)	Nicotinamide adenine dinucleotide phosphate
[NiFe]-H_2ase	Nickle iron hydrogenase
Nudix	Nucleotide diphosphate linked to some X
PEMFC	Proton exchange membrane fuel cells
PHI	6-phospho-3-hexuloisomerase
PMSF	α-toluenesulfonyl fluoride
PQQ	Pyrroloquinoline quinone
RET	Renewable energy technologies
RH	*Wautersia eutropha* regulatory hydrogenase
RuMP	Ribulose monophosphate
SDS-PAGE	SDS-polyacrylamide gel electrophoresis
SH	*Wautersia eutropha* soluble NAD$^+$-dependent hydrogenase
SOEing	Splicing by overlap extension PCR method
Tris-HCl	2-Amino-2-(hydroxymethyl)-1,3-propanediol hydrochloride

Chapter 1. General Introduction

1.1. General problem

The state of the global economic and political stability is influenced by fossil fuel resource distribution. Eighty percent of the present world energy demand is supplied by fossil fuels. This near-strict dependence on fossil fuels has lead to negative changes in the global climate (Wuebbles and Jain, 2001), the environment (Momirlan and Veziroglu, 2005), and human health (Davis, 1997; Clauss *et al.*, 2005). These climate changes are primarily due to incomplete combustion of fossil fuels resulting in air pollutant emissions like CO_x, NO_x, SO_x, C_xH_x, soot, ash, droplets of tar, and many more organic compounds (Das and Veziroglu, 2001).

1.2. The Kyoto Accord and the Canadian commitment

Over the last three decades there has been renewed interest in renewable energy technologies (RET) in Canada, mainly due to sharp increases in the price of oil during the late 1970s and early 1980s, and more recently the need to meet the Kyoto targets of reducing CO_2 and greenhouse gas emissions by 6 % below 1990 levels by 2012. World interest in RETs can be seen in the increasing global market share, which is currently worth approximately of US$ 6.78 billion, and is expected to grow to US$ 82 billion by the year 2010. Today, renewable energy sources account for more than 14 % of the total energy demand. Due to its rich natural resources and geography, Canada meets more than 64 % of its 69,809 mega watt yearly needs with hydroelectric power. However, Canada as a nation faces some real challenges to reduce CO_2 and greenhouse gas emissions. As a result of extreme climate,

geographical size, and its industries' energy-intensive nature, Canada has one of the highest annual energy consumptions among industrial nations. In 2002, the Canadian commercial consumption of oil was 288.7 million tones of oil equivalents and Canadian citizens had the highest energy consumption per capita of any industrial nation accounting for of about 21 tones of greenhouse gases per year per capita (Islam *et al.*, 2004).

1.3. Climate change action plan

To meet the Kyoto target, the Canadian government has formulated the Climate Change Action Plan. This Climate Change Action Plan aims to reduce the rate of green-house gas emissions by investing in abatement technologies, including RETs, and simultaneously deregulating and restructuring the electrical energy sector. These two actions are expected to promote competition in the energy retail markets and give customers more choice. With more retail competition and choice, it is anticipated that there will be an increased interest in, and use of, renewable energy sources from RET (Islam *et al.*, 2004).

RETs do not generate energy directly but convert renewable sources of energy to useful energy vectors or carriers. Green power technologies are an attractive alternative to most traditional means of power production. In contrast to most fossil fuel plants, large hydro dams, or nuclear plants that can take several years to develop, most green power technologies can deliver power within a relatively short timeline.

Nearly half of all emissions in Canada are attributed to emissions from internal combustion engines from automotive vehicles (Potoglou & Kanaroglou, 2005). Most of the proposed green alternative power systems are large static stations,

and therefore, the technology cannot be directly transferred to the automobile. The energy generated by these green technologies, mostly as electricity, can be stored in batteries. However, battery technology cannot store sufficient energy to meet current automotive needs (Bitsche & Gutmann, 2004). Although green fuel technology can easily be transferred to the automobile, green fuels emit emissions as well, albeit at lower emission levels than fossil fuels (Lapuerta *et al.*, 2005). Therefore, most of the green alternative power systems proposed will be largely ineffective in reducing greenhouse emissions.

1.4. Hydrogen

Hydrogen gas is thought to be the ideal fuel to alleviate air pollution, arrest global warming, and protect the environment in an economically sustainable manner (Johnston *et al.*, 2005). The direct combustion of hydrogen and oxygen is highly energetic. However, the homolytic cleavage of hydrogen needs energy, thus preventing a reaction at ambient temperatures without a catalyst. In proton exchange membrane fuel cells (PEMFC), hydrogen and oxygen react not in a direct combustion but in a cold electrolyte mediated process, and unlike batteries, they are almost endlessly rechargeable. These electrochemical cells constitute an attractive power generation technology that converts chemical energy into electricity, where the fuels (hydrogen, hydrocarbons, or alcohols) react directly, and with high efficiency with an oxidant (oxygen). When pure hydrogen is used in these cells, the combustion product is just water (Boettner & Moran, 2004). However, storage and distribution of hydrogen is problematic, as the liquefaction of gaseous hydrogen for ease of storage is energy intensive and therefore costly and the transportation of potentially explosive

gaseous hydrogen is dangers, prompting interest in the development of other fuels (Ananthachar & Duffy, 2005).

1.5. Methanol as a Source of Hydrogen

Liquid fuels are preferred over gaseous fuels for mobile applications. Methanol is an ideal candidate as a liquid fuel substitute to hydrogen gas because of the following reasons: (1) methanol can be made from both fossil (e.g., natural gas) and renewable energy sources (e.g., biomass; Chmielniak & Sciazko, 2003), (2) it remains liquid under standard temperatures and pressures, (3) methanol can be distributed and stored using existing fossil fuel infrastructure and (4) it is relatively hydrogen dense.

Hydrogen is produced from methanol at an industrial scale by passing a stream of methanol over metal catalysts at high temperatures. Carbon monoxide, also generated in this process, is subsequently removed via a gas purification system. The pure hydrogen is then usable in PEMFC hydrogen fuel cells. However, hydrogen production by thermocatalytic reformation of methanol has drawbacks. The process is costly, because external heat sources are required to generate the high temperatures needed for the reforming process. The reformer is also physically bulky, limiting the use of reformers in mobile fuel cell applications (Peppley *et al.*, 1999).

1.6. Biotechnology and Hydrogen Production

There are clear advantages to the potential use of PEMFC as an alternate source of clean renewable energy. However, the major limitations to overcome before this technology will have wider use are the difficulties in storing, transporting (Ananthachar & Duffy, 2005), and producing hydrogen (Peppley *et al.*, 1999). To

address these limitations, two branches of research have emerged that take advantage of the inherent advantages of microbial biological systems and enzyme biocatalysts for the biological production of hydrogen.

The biological production of hydrogen or biohydrogen is an attractive alternative hydrogen-producing technology because it offers several advantages over traditional chemical reformation processes: (1) Hydrogen is produced at ambient temperatures and pressures, making the process less energy intensive and, therefore, more cost effective; (2) A wide range of renewable materials can be used to generate hydrogen (e.g., glucose and waste paper); and (3) The biocatalysts used to produce hydrogen are renewable (Das & Veziroglu, 2001).

1.7. Microbial Production of Hydrogen

Microorganisms utilize a variety of metabolic strategies to produce hydrogen, including direct biophotolysis, indirect biophotolysis, photo-fermentation, water-gas shift reaction, and dark fermentation (Nandi & Sengupta, 1998; Das & Veziroglu, 2001; Levin *et al.*, 2004). Of these metabolic strategies, mixed cultures of mostly *Clostridium* bacteria species have the highest observable rate of hydrogen production during dark fermentation when grown in carbohydrate-rich substrates under bioreactor conditions. The theoretical rate of hydrogen produced by a bioreactor of approximately 100 L would is sufficient to fuel a PEMFC that could provide electric power for an average non-electrically heated house in British Columbia (Levin *et al.*, 2004).

The microbial produced of hydrogen does have advantages. The potential reuse of waste products such as paper as a source of hydrogen is attractive. However,

the production of hydrogen by microbes has limitations because hydrogen production is tied to the complex metabolism of the microorganism. During the production of hydrogen, a mixture of gases is produced, including CO_2 that will poison the metal catalysts in PEMFC resulting in a reduced electrical power density. To prevent these poisoning effects, these additional gases must be removed by the same gas purification systems used in the chemical reformation of hydrogen. Consequently, microbial production of hydrogen suffers the same drawbacks as the chemical reformation of hydrogen. Hydrogen production by microbes is also dependent on specific growth conditions, such as light intensity, pH, temperature, and nutrient content, that are in constant flux during the growth of micro-organisms. As a result, sophisticated bioreactors are required to maintain these optimal growth conditions, adding to the cost of producing hydrogen by microbes. In addition, the hydrogen that is produced must be constantly removed if continuous hydrogen production is to be achieved. If the hydrogen is permitted to accumulate, the metabolism of the organism will shift away from the production of hydrogen. Again, sophisticated bioreactors and gas purification systems are required to maintain optimum hydrogen gas concentrations for continuous hydrogen production. Metabolic by products occur during the production of hydrogen. These drive competing metabolic pathways that diminish hydrogen production (Levin *et al.*, 2004).

1.8. Enzymatic production of hydrogen

Chemical catalysts, typically transition metals, play a crucial role in many aspects of industrial and human progress from the efficient manufacture of materials to the creation of new energy sources. However, the application of biotechnology to

industry has introduced a shift to the use of biological catalysts because they offer several advantages due to their intrinsic nature. Generally, biological catalysts are more environmentally friendly than their chemical counterparts. This is partly due to the mild conditions (low temperature and low pressure) at which chemical reactions are catalyzed. Biological catalysts are also generated from renewable sources and are biodegradable. In contrast, the recycling or deposition of transition metal catalysts can constitute a major environmental problem. Biological catalysts also catalyze reactions in aqueous solutions at near neutral pH, avoiding the use of potentially hazardous organic solvents. Because reaction conditions (temperature and pH) are relatively the same, biological catalysts can be used in high-yield multi-step processes, due to the elimination of intermediate synthetic steps and solvent switching. The reactions of biological catalysts are also very specific, preventing the production and accumulation of side-products. Finally, an expanding range of substrates can be utilized as the number of known biocatalysts increases (Burton, 2001).

Woodward *et al.* (2000) described the *in vitro* production of hydrogen from glucose using the nicotinamide adenine dinucleotide phosphate [NADP(H)]-dependent enzymes glucose dehydrogenase (GDH) from *Thermoplasma acidophilum* and the hydrogenase from *Pyrococcus furiosus* (Pfu H_2ase) from archea bacteria. The data presented by Woodward *et al.* (2000) suggested that hydrogen gas was produced by the electron flow from the oxidation of glucose by GDH to the Pfu H_2ase via continuous recycling of the co-factor $NADP^+$. The continuous cycling of $NADP^+$ / NADPH results in continual evolution of H_2 gas at stoichiometric yields.

The enzymatic production of hydrogen offers two advantages over the microbial production of hydrogen. Firstly, enzymatic production of hydrogen provides a predictable pathway of fuel oxidation as the enzymes used in the reactions are selected. The ability to select enzymes allows determination of the reaction conditions and prediction of by-product generation, allowing for a more flexible hydrogen-producing system that is easy to manipulate. Secondly, the enzymatic production of hydrogen generates higher yields of hydrogen because there are no additional enzyme pathways competing with H_2 production.

1.9. *In vitro* production of hydrogen from methanol

The work by Woodward *et al.* (2000) suggests a new pathway for the coupled-enzyme conversion of hydrogen from renewable resources. However, the proposed enzyme conversion of hydrogen from glucose has two main limitations.

Glucose has a low hydrogen to mass ratio, therefore, making glucose a poor biological storage molecule for hydrogen. Methanol has the high hydrogen to mass ratio (6 %) making methanol an efficient hydrogen storage molecule as compared to glucose (1 %). Methanol can also be oxidized by a variety of NAD-dependent alcohol dehydrogenases, by the following reaction.

$$CH_3OH + NAD^+ \rightarrow CHO + NADH + H^+ + 2e^-$$

The NAD-dependent methanol dehydrogenase from *Bacillus methanolicus* C1 (BmMDH) has been shown to have the highest methanol oxidation rates among NAD-dependent alcohol dehydrogenases (De Vries *et al.*, 1992; Hecktor *et al.*, 2002).

Secondly, work by Woodward *et al.* (2000) used the oxygen sensitive nickel iron hydrogenise ([NiFe]-H_2ases) from *Pyrococcus furiosus*. To obtain active oxygen-sensitive [NiFe]-H_2ase, the purification of [NiFe]-H_2ase is performed under anaerobic conditions requiring the use of expensive and specialized equipment (Cammack et. al, 2001). In contrast, the soluble NAD-dependent hydrogenase (SH) from *Wautersia eutropha* is oxygen insensitive (Schneider & Schlegel, 1976). Therefore, allowing the purification of the enzyme in aerobic conditions without the use of expensive and specialized equipment.

In conclusion, the bioconversion of molecular hydrogen from oxidation of methanol using *Wautersia eutropha* NAD-dependent hydrogenase, and *B. methanolicus* C1 methanol dehydrogenase would over come the limitations of system proposed by Woodward *et al.*, (2000; Figure 1).

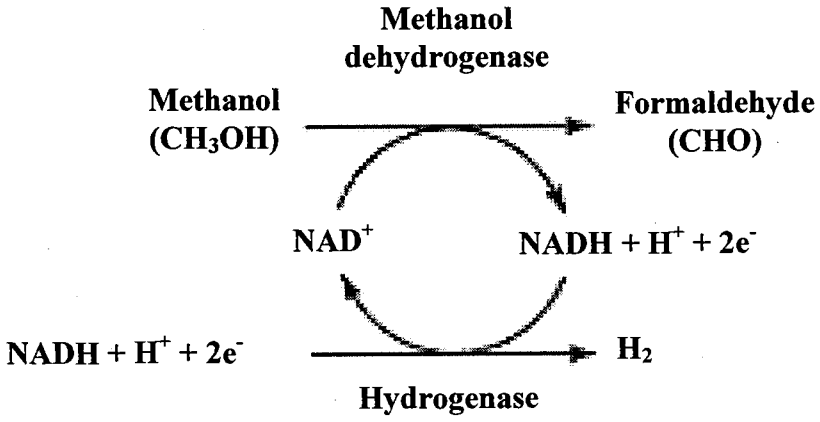

Figure 1: Coenzyme conversion of methanol to formaldehyde via oxidation of methanol to formaldehyde by *Bacillus methanolicus* C1 methanol dehydrogenase and the recycling of the coenzyme via oxidation of reduced NAD^+ by *Wautersia eutropha* soluble hydrogenase.

Chapter 2. *Bacillus methanolicus* C1 Methanol Dehydrogenase

In nature, methanol is formed from the methyl esters and ethers from plant components such as pectin and lignin. The methylotrophic micro-organisms are able to grow on methanol and have been isolated from soil samples. *Bacillus methanolicus* C1 belongs to a clade of obligate aerobic, thermotolerant Gram-positive bacteria that can grow at temperatures of 35 °C to 65 °C, with optimum growth at 55 °C (Arfman *et al.*, 1992). Previous work studying the methanol metabolism of *B. methanolicus* C1 (Arfman *et al.*, 1991), provided evidence for the presence of a novel type of methanol oxidizing enzyme (MDH) involved in the metabolism of primary aliphatic alcohols in this organism.

2.1. Methanol metabolism in bacteria

Methylotrophic organisms use one-carbon compounds (e.g., methane, methanol, methylamine) for growth. Several specific pathways for assimilation of one-carbon substrates have been determined in different aerobic methylotrophs (Arfman *et al.*, 1989). Carbon-carbon bonds are formed from these pathways, generating compounds that serve as building blocks for synthesis of cell-material.

Methylotrophic bacteria generate the metabolic energy required for growth by dissimilating methanol to CO_2. Two different routes for methanol dissimilation are known, the linear pathway and the dissimilatory RuMP cycle (Arfman *et al.*, 1989). The linear pathway involves the oxidation of methanol via formaldehyde and formate to CO_2. In contrast, the metabolic energy and carbon fixation in Gram-positive bacteria is facilitated through the ribulose monophosphate (RuMP) pathway during growth on methanol (Dijkhuizen *et al.*, 1988).

Methanol is initially oxidized to formaldehyde that then enters the RuMP cycle via the fixation of formaldehyde with ribulose-5-phosphate to form fructose-6-phosphate catalyzed by 3-hexulose-6-phosphate synthase (HPS) and 6-phospho-3-hexuloisomerase (PHI). Fructose-6-phosphate is then used as a substrate for carbon fixation via the Embden-Meyerhof pathway or as a substrate for metabolic energy. Metabolic energy is generated from the electron transport chain using NADH (Arfman *et al.*, 1989). The electrons from the reduced NADH are then donated to the electron transport chain at or above the cytochrome b level (Dijkhuizen *et al.*, 1988). Energy can also be generated via glycolysis by the conversion of fructose-6-phosphate. To complete the RuMP cycle, ribulose-5-phosphate is regenerated from fructose-6-phosphate and glyceraldehyde-3-phosphate (Arfman *et al.*, 1989).

2.2. Enzymes oxidizing primary alcohols

The oxidation of oxidizing primary alcohols is catalyzed by at least three distinct types of enzymes. In yeast, an FAD-dependent peroxisomal alcohol oxidase enzyme catalyzes the oxidation of methanol to formaldehyde and hydrogen peroxide using oxygen as an electron acceptor (Harder & Veenhuis, 1989). Gram-negative methylotrophic bacteria oxidize methanol with a pyrroloquinoline quinone (PQQ) dependent methanol dehydrogenase (EC 1.1.99.8) that is localized in the periplasmic space. The periplasmic localization of the PQQ-dependent methanol dehydrogenase protects other cellular components from the toxic nature of formaldehyde, the metabolic product of methanol oxidation (Anthony, 1986).

In contrast, Gram-positive bacteria generally possess NAD-dependent alcohol dehydrogenase (Arfman *et al.* 1997). Three families of NAD-dependent alcohol

dehydrogenases (ADH) have been characterized based on the molecular weight of the enzyme. The most common form of ADH is the Type I or medium-chain length ADH. While not as abundant, the short-chained Type II ADHs and long-chained Type III ADHs are also found in many organisms (Littlechild *et al.*, 2004). The Type III ADHs are distinct from the zinc-containing medium-chained Type I and the zinc-lacking short-chained Type II ADHs. The initial members of the Type III were iron-dependent ADHs. Over time, as more Type III alcohol dehydrogenases were characterized, it was realized that not all members contained iron. Several proteins contained other metal atoms, such as zinc and magnesium, instead of iron (Reid & Fewson, 1994).

2.3. *Bacillus methanolicus* C1 methanol dehydrogenase

The methanol dehydrogenase of *Bacillus methanolicus* C1 (BmMDH) is a Type III ADH (De Vries *et al.*, 1992) nicotinoprotein alcohol dehydrogenase consisting of 10 identical subunits of M_r 43,000 each. The subunits are arranged in five-fold mirror symmetry with a diameter of 15 nm (Vonck *et al.*, 1991). Each subunit also contains one Zn^{2+} ion and one or two Mg^{2+} ions and one tightly bound NAD(H) cofactor to each monomer subunit (Hektor *et al.*, 2002). The BmMDH has been purified to homogeneity under aerobic conditions from cells grown in both methanol-limiting conditions (Arfman *et al.*, 1989) and from over-expressed in *E. coli* (cMDH; De Vries *et al.*, 1992). BmMDH activities of *Bacillus methanolicus sp.* C1 cytoplasmic extracts grown under methanol-limiting conditions at optimal conditions (50 °C, pH 9.5) displayed an activity of 1000-1200 $nmol.min^{-1}.mg^{-1}$ of protein. The

activity of BmMDH is also strongly stimulated by the presence of Mg^{2+} and an activator protein (Arfman *et al.*, 1997).

The *B. methanolicus* C1 possesses a soluble M_r 27,000 activator protein that stimulates the relatively low activity of BmMDH towards methanol. This stimulation is $Mg2^{+}$-dependent and results in a 40-fold increase in BmMDH turnover rate. The activator protein belongs to the family of Mg^{2+} dependent Nudix (nucleotide diphosphate linked to some X) hydrolyze (Bessman *et al.*,1996; Kloosterman *et al.*, 2002). The activator protein acts independently to the catalytic mechanism, as the velocity maximum (V_{max}) of formaldehyde reductase activity remains unchanged (Arfman *et al.*, 1991). *In vivo* this protein may have an important physiological role, contributing to the control of BmMDH activity. BmMDH is synthesized in abundant amounts and consist of up to 22% of total soluble protein (Arfman *et al.*, 1989), making its control a delicate problem since accumulation of formaldehyde, the product of the BmMDH reaction, is lethal to the cell (Arfman *et al.*, 1992).

2.4. Nicotinoproteins

NAD(P) functions as a coenzyme for a large variety of dehydrogenase enzymes, receiving or donating electrons depending on the specific reaction catalyzed and the reaction conditions. The cytosolic NAD(P)(H) can be oxidized or reduced elsewhere in the cell, e.g., by NAD(P)-dehydrogenase in the cytoplasmic membrane. BmMDH is a unique NAD(P)-nicotinoprotein that possesses a tightly bound NAD(P)(H) that remains bound during catalysis. The rate of BmMDH activity can also be increased by the presence of an activator protein (Hektor *et al.*, 2002).

In the non-activated state, the reducing equivalents resulting from methanol oxidation are transferred via a ping-pong type of mechanism. Reducing equivalents from methanol are transferred to an exogenous coenzyme NAD^+ via the bound cofactor NAD(H). However, during activation, the activator protein removes the nicotinamide moiety from the tightly bound NAD(H) cofactor in a Mg^{2+}-dependent hydrolysis reaction. The removal of the nicotinamide moiety allows the exogenous coenzyme NAD^+ to occupy the partially vacant NAD(H) cofactor site, permitting a direct exchange of reducing equivalents between the exogenous NAD(H) and the BmMDH active site, resulting in a ternary complex mechanism (Hektor *et al.*, 2002).

2.5. Alcohol dehydrogenase NAD-binding

Alcohol dehydrogenase enzymes oxidize alcohols by transferring a hydride-ion from the carbon atom that binds the hydroxyl group (OH), and a proton from the OH group, to an oxidized coenzymes or cofactors. To allow direct hydrogen transfer to occur, both the alcohol substrate and the coenzyme/ cofactor must bind in the correct orientation within the enzyme active. The dinucleotide binding domains of various dehydrogenases have very similar three-dimensional structures, although the amino acid side-chains that interact with NAD(P) can vary (Lesk, 1995).

The amino acid sequence of the *B. methanolicus* C1 MDH has significant sequence similarities with the iron-containing Type III ADH, among these is a specific nicoprotein-binding domain, Motif A ($GGGSX_2DX_2K$). The amino acid residues Gly95, Ser97, Asp100, and Lys103 in BmMDH of Motif A are highly conserved and have important roles in cofactor binding (Hektor *et al.*, 2002). The NAD cofactor is tightly bound to the BmMDH apo-protein by hydrogen bonds

between the Gly95 residue and the 2'-hydroxyl group of the adenine ribose and the hydroxyl group of the Ser97 and the 2'-phosphate group of the NAD(H) cofactor. In addition, the Asp100 and Lys103 residues are thought to be hydrogen bonded to the carboxyamine group of the NMN(H) of the NAD(H), aiding in the positioning of cofactor within the active site. The Motif A also displays sequence similarity to alcohol oxidase FAD-binding domain of *Hansenula polymorpha* ($DIIVVGGGSX_{22}E$). In addition, the alcohol oxidase FAD-binding domain of *Hansenula polymorpha* functions as a cofactor and remains tightly associated with the apo-protein during catalysis. This tight association of the cofactor to the apo-protein is similar to the association of NAD(H) cofactor found in BmMDH (Hektor *et al.*, 2002). Also characteristic to Type I ADH NAD-dependent enzymes is a highly conserved NAD(P)-binding dinucleotide-binding domain, or Rossmann-fold. The fingerprint for this binding domain is "GXGXX(G/A)" the dinucleotide-binding domain consists of a βαβ fold in the secondary structure. The three Gly residues are thought to be critical to efficient coenzyme binding. The first Gly residue is involved in forming the first tight βα turn. The second Gly residue has been implicated in the binding of the dinucleotide. The third Gly residue allows a close interaction between the β strands and the α helix. The coenzyme is positioned within this fold such that the 2'-OH of the adenosine ribose moiety forms hydrogen bonds with a conserved Asp or Glu residue (Wierenga *et al.*, 1986).

In contrast, the Type III ADHs have an imperfect fingerprint (GXG) found in the N-terminal part of the protein. The two Gly residues also appear to have no direct involvement in the binding of the cofactor as observed in mutational analyzes.

However, mutation of the conserved Asp residue leads to binding deficiencies in both the cofactor and coenzyme and results in an inactive NAD(H) deficient mutant. Despite the partial fingerprint, the modified NAD(P)-binding domain allows for tight binding of the coenzyme (Hektor *et al.*, 2002).

2.6. Mutational analysis of *B. methanolicus* C1 methanol dehydrogenase NAD-binding

Mutational analyses implicate the importance of Ser97 on binding of the NAD(H). The Ser97 mutant resulted in a BmMDH that did not rely on the activator protein for efficient methanol dehydrogenase activity. In wild type BmMDH, the hydrogen bond between the hydroxyl group of Ser97 and the 2'-phosphate group of the NAD(H) cofactor plays an important role in the tight binding of the cofactor to the apo-enzyme. In the Ser97 to Gly97 mutant (S97G), the hydrogen bond is lost, and the NAD(H) cofactor is no longer bound to the apo-protein. However, the NAD(H)-cofactor site of the S97G mutant still has affinity for NAD(H) and now functions as a NAD(H)-coenzyme site. Although the binding of the NAD(H) coenzyme to the BmMDH apo-protein would be different than the activated BmMDH, the binding of the NAD(H) coenzyme is in the correct orientation. As a result, methanol oxidation in the mutant BmMDH S97G proceeds via a coenzyme-dependent ternary reaction mechanism without the presence of the M_r 50,000 activator protein at a reaction rate that is 10 times greater than the activated wild type BmMDH (Hektor *et al.*, 2002).

Chapter 3. *Wautersia eutropha* soluble Ni-Fe hydrogenases

Molecular hydrogen is widely utilized as a substrate by micro-organisms. Many microbes can generate reducing power by hydrogen oxidation, while others can release excess reducing equivalents in the form of dihydrogen. Microbes metabolize molecular hydrogen via hydrogenases (H_2ase) that catalyze the bi-directional reaction: $H_2 \leftrightarrow 2H^+ + 2e^-$ (Vignais *et al.*, 2001).

Although most H_2ase are able to catalyse this reaction bi-directionally, H_2ases will only catalyses either H_2 uptake or H_2 evolution *in vivo*, depending on the redox balance within of the organism. For example, clostridial bacteria use H_2ase as a means of disposing excess reducing equivalents (Adams *et al.*, 1981), while H_2 is used as a source of energy as in photosynthetic bacteria (Vignais *et al.*, 1985). The localization of H_2ases also varies. Hydrogen uptake H_2ases are often localized in the periplasmic space or cell membrane, while H_2 synthesis is most often localized in the cytoplasm. However, some cytoplasmic bi-directional hydrogenases also function as hydrogen uptake mediators. The number and types of H_2ases utilized by organisms can vary with some bacteria having more than one H_2ase localized in different cell compartments. Due to the complexities of function and localization, as well as the structural complexity of the synthesis of the active sites, H_2ases require many accessory genes for correct assembly, insertion, and activity (Vignais *et al.*, 2001).

Hydrogenases were traditionally studied using well-established physiological and biochemical techniques. As a result, the study of hydrogenases was first limited to aerobic hydrogen oxidizing prokaryotes of the domain Eubacteria (Adams *et al.*, 1981). H_2ases have also been studied from the Archeabacteria (Graf *et al.*, 1981),

specifically *Euryarchaeota* and the *Crenarchaeota*, in which many species rely on H_2 as an energy source (Woese, 1994). More recently, H_2ases have been found in subcellular organelles of eukaryotes, specifically the hydrogenosomes of protozoa (Muller, 1993) and chloroplasts of green algae (Vignais *et al.*, 2001).

3.1. Classification of metalloenzyme hydrogenases

The majority of H_2ases are classified as metalloenzymes with only a few H_2ases having no metal in their catalytic active sites. H_2ase metalloenzymes are classified into two categories based on the type of metal ions at their catalytic sites. The first consists of [2Fe-2S], [3Fe-4S], and [4Fe-4S] iron-sulphur clusters. The metal sites shuttle electrons between the H_2-activating sites and the redox partners of H_2ases. The second type of metal clusters contains only Fe or Ni-Fe. Fe-containing H_2ases are very sensitive to oxygen, while Ni-Fe H_2ases may be oxygen tolerant (Vignais *et al.*, 2001).

3.2. [Ni-Fe] hydrogenases

In Proteobacteria, the structural genes of H_2ase are typically clustered and are located either on the chromosome of the bacterium or on a mega plasmid. The genes involved in H_2ase maturation are denoted alphabetically in order of occurrence within an operon and are typically downstream of the H_2ase structural genes. A set of maturation genes (*hyp*; hydrogen pleiotropic genes) are also found in these loci and are required for the insertion of nickel (Ni), iron (Fe), carbon monoxide (CO) and cyanide (CN) into the active sites of the structural proteins (Casalot and Rousset, 2001). Mutations in any of the *hyp* genes have a pleiotropic effect on the H_2ase, leading to a substantial decrease or a complete loss of enzymatic activity due to a

failure to assemble the [Ni-Fe] active site (Dernedde *et al.*, 1996). Finally, H_2ase gene clusters contain regulatory genes that control the expression of the structural genes (Friedrich *et al.*, 2005).

3.2.1. Basic structure of [Ni-Fe] hydrogenases

Based on x-ray crystallography data from the model Ni-Fe-H_2ase from *Desulfovibrio gigas*, Ni-Fe-H_2ases are heterodimers comprised of a large and small subunit. The large 60 kDa subunit of *D. gigas* contains the bimetallic [Ni-Fe] catalytic site with one nickel and one iron atom linked to the protein by four cysteic thiolates. The Ni atom of the metal active site is coordinated in a highly distorted square pyramidal conformation by a pair of thiol groups from N- and C-terminal cysteines with a vacant sixth axial ligand site. The Fe atom is coordinated by six ligands in a distorted octahedral conformation that shares one thiol group from each cysteine pair and is coordinated by one CO and two CN^- diatomic non-protein ligands (Volbeda *et al.*, 1995; Fontecilla-Camps *et al.*, 1997).

The small subunit contains two domains. The N-terminal domain contains a highly conserved binding pocket for the proximal [4Fe-4S] cluster, while the C-terminal contains a highly variable region for the binding pocket for the middle and distal [Fe-S] clusters. The large and small subunits have extensive surface contacts and are anchored together by approximately 25 side chains. As a result of this interaction, the active site is buried deep within the H_2ase situated between the large subunit and the proximal [4Fe-4S] cluster of the small subunit (Volbeda *et al.*, 1995).

3.2.2. Catalysis of hydrogen at the NiFe active site

The oxidation of hydrogen by the active site of NiFe hydrogenase is a heterolytic process resulting in the creation of a hydride and a hydron. The resulting hydride then donates two electrons to the [4Fe-4S] clusters. Fe-S clusters, however, can only accept one electron at a time, and it is energetically unfavorable to have a $H^{\bullet}$ intermediate step. This is in contrast to other redox partners like NAD^{+} or FMN that can accept two electrons at one time. To compensate for this discrepancy, the catalysis of hydrogen involves a reaction cycle where the metal active site accepts two electrons from the hydride simultaneously and then passes off the electrons one at a time to the proximal [4Fe-4S] cluster (Cammack *et al.*, 2001).

Under aerobic conditions, the Ni-Fe-H_2ase is inactive and unable to accept H_2 molecules at the metal active site. This is due in part to an O_2 atom bound to the available six-coordinated site of the [Ni-Fe] active site under aerobic condition and not to protein denaturing effects. The oxidized inactive Ni-Fe-H_2ase can be converted to an active and ready state by reducing O_2 to OH^{-}, followed by protonation to H_2O and finally removal from the active site. In this state, the active site is charge neutral:

$$Fe^{(II)}\text{-}Ni^{(II)} + [4Fe\text{-}4S]^{2+}$$

Upon further reduction, the electron/proton combines with the Ni atom reducing the oxidative state of the NiFe center:

$$(1)\ Fe^{(II)}\text{-}Ni^{(III)} + e^{-} + H^{+} + [4Fe\text{-}4S]^{2+} \rightarrow Fe^{(II)}\text{-}Ni^{(II)}(H^{+}) + [4Fe\text{-}4S]^{2+}.$$

The proximal [4Fe-4S] cluster then quickly oxidizes the Ni atom:

$$(2)\ Fe^{(II)} - Ni^{(II)}(H^+) + [4Fe\text{-}4S]^{2+} \rightarrow Fe^{(II)} - Ni^{(III)} + [4Fe\text{-}4S]^{1+}.$$

During the oxidation of the Ni atom, an H_2 molecule binds to the Fe atom. To maintain a charge neutral state, a hydron is released from H_2 and is transferred to a base moiety (B) near the reduced [4F-4S] cluster, leaving the a hydride on the electron-deficient Fe atom:

$$(3)\ Fe^{(II)} - Ni^{(III)} + [4Fe\text{-}4S]^{1+} + \mathbf{H_2} \rightarrow \mathbf{(H)}Fe^{(II)} - Ni^{(III)} + [4Fe\text{-}4S]^{1+} + \mathbf{BH^+}.$$

The proximal cluster then donates its single electron to an external electron acceptor (EA):

$$(4)\ (H)Fe^{(II)} - Ni^{(III)} + [4Fe\text{-}4S]^{1+} + EA \rightarrow (H)Fe^{(II)} - Ni^{(III)} + [4Fe\text{-}4S]^{2+} + \mathbf{EA^{1-}}$$

Both electrons from the hydride are temporarily transferred to the Ni atom reducing the Ni(III) to Ni(I):

$$(5)\ \mathbf{(H)}Fe^{(II)} - Ni^{(III)} + [4Fe\text{-}4S]^{2+} \rightarrow Fe^{(II)} - Ni^{(I)} + [4Fe\text{-}4S]^{2+}.$$

One electron from the reduced Ni atom is transferred to the proximal [4F-4S] cluster resulting in an oxidized but active Ni(II):

$$(6)\ Fe^{(II)} - Ni^{(I)} + [4Fe\text{-}4S]^{2+} \rightarrow Fe^{(II)} - Ni^{(II)} + [4Fe\text{-}4S]^{1+}.$$

Finally, a second electron is transferred to the external electron acceptor regenerating the catalytically active metal site (Cammack *et al.*, 2001):

$$(7)\ Fe^{(II)} - Ni^{(II)} + [4Fe\text{-}4S]^{1+} + \mathbf{EA}^{1-} \rightarrow Fe^{(II)} - Ni^{(II)} + [4Fe\text{-}4S]^{2+} + \mathbf{EA}^{2-}$$

3.2.3. Electron transfer

Unlike many enzymes that readily undergo conformational changes when binding its substrate, the active site of H_2ases are deep within the protein, encased in a rigid structure. To facilitate the delivery of the substrate to the active site, H_2ases possess internal network of hydrophobic channels to direct the small hydrogen molecules to the Ni atom at the catalytic metal center deep within the large subunit (Volbeda *et al.*, 1995). Upon heterolytic cleavage of hydrogen, electrons in the form of hydride ions are transferred in series of discrete 1.0-1.5 nm steps from the Ni atom to the proximal Fe-S cluster, then through the middle, where a hydron is stripped, and finally to the distal Fe-S clusters of the H_2ase small subunit. Because electrons can tunnel out of proteins during these discrete steps, it has been postulated that the deep active site prevents unwanted reduction of components found at the surface of the protein (Page *et al.*, 1999). Electrons liberated from the large subunit catalytic site are transferred to variety of electron acceptors and donors via the small subunit Fe-S

clusters. These electron acceptors and donors include cytochromes, ferredoxins, or NAD^+ that may interact indirectly with the hydrogenase through multimeric redox subunits of the H_2ase (Montet *et al.*, 1997).

3.3. Soluble [Ni-Fe] hydrogenase of *Wautersia eutropha*

The β-proteobacterium *Wautersia eutropha* strain is one of best-studied facultative chemolithoautrophic bacterium. *W. eutropha* uses organic substances as a source of carbon and energy. In the absence of organic substrates, however, *W. eutropha* can assimilate CO_2 as the sole source of carbon. The assimilation of CO_2 is driven by a hydrogen energy conservation system involving two H_2ases; a soluble NAD^+-dependent hydrogenase (SH), and a membrane-bound H_2ase (MBH). The H_2ases of *W. eutropha* are also unique, as the SH and MBH can oxidize hydrogen under aerobic conditions (Schneider & Schlegel, 1976).

W. eutropha complex metabolism is reflected in its complex genome comprised of three independent replicons: Chromosome 1 (4.05 Mbp), chromosome 2 (2.90 Mbp), and mega-plasmid pHG1 (0.45 Mbp). The mega-plasmid pHG1 is self-transmissible and harbors the genes for the following metabolic processes: (1) H_2-metabolism, (2) CO_2-fixation, (3) anaerobic metabolism via denitrification, (4) iron uptake, and (5) the degradation of aromatic substances (Schwartz *et al.*, 2003). To survive in variable hydrogen environments, *W. eutropha* has evolved oxygen-tolerant H_2ases and the regulatory ability to sensitively detect H_2 and rapidly adapt to changing organic material supply (Friedrich *et al.*, 2005). The plasmid-linked genes for H_2-oxidation are localized in three well-defined operons containing both the structural genes, the accessory genes for post-translational metallocentre assembly,

and the regulation for three distinct [NiFe]-H_2ases. The first is a trimeric, membrane-bound enzyme (MBH) that couples H_2 oxidation to electron transport phosphorylation via a dependent cytochrome b-type membrane anchor (Bernhard *et al.*, 1996). The second is a soluble hetrotetrameric H_2ase (SH) that reduces NAD^+ as the physiological electron acceptor for the sequestering of CO_2 (Massanz *et al.*, 1998). The third is a soluble oligomeric regulatory hydrogenase (RH; Friedrich *et al.*, 2005). The MBH will not be mentioned further, and the focus will be placed on the SH and the RH of *W. eutropha.*

3.3.1. Biochemical characteristics

The soluble NAD^+-dependent [NiFe] hydrogenase of *W. eutropha* H16 has been purified to homogeneity under anaerobic conditions. The molecular weight and isoelectric points have been determined to be 205 kDa and 4.85 pI, respectively. The isolated H_2ase is in an oxidized, highly stable, but non-reactive state. The H_2ase can be activated by the addition of either reducing agents or catalytic amounts of NADH. However, the active form of H_2ase is unstable and loses activity within 5 days in the presence of 5 μm NADH (Schneider & Schlegel, 1976). In addition to H_2ase activity, SH also possesses diaphorase activity.

The rate of reduction of NAD^+ in the presence of saturated levels of H_2 is observed to be 50 μmol H_2/min mg of protein, with an apparent Michaelis constant (K_m) of 0.037 mM. The K_m for NAD^+ was found to be 0.56 mM in reductively pre-treated SH. The H_2 evolution rate from NADH was determined to be 1.2 μmol H_2/ min per mg of protein or approximately 2.5% of the reverse reaction in reductively pre-treated SH (Schneider & Schlegel, 1976).

3.3.2. Structural genes arrangement

The H_2ase gene cluster of *W. eutropha* spans 80 kbp in the 450 kb mega-plasmid pHG1 in two distinct operons, *hoxS* and *hoxM*, encoding the SH and MBH respectively (Tran-Betcke *et al.*, 1990; Schwartz *et al.*, 2003). The four structural genes of SH, *hoxFUYH*, are tightly linked within a 5 kb region of pHG1. The structural genes for the diaphorase moiety, *hoxF* and *hoxU,* overlap at their respective start and stop codons. The genes *hoxU* also overlaps *hoxY* at their respective stop and start codons. The structural genes for the hydrogenase moiety, *hoxY* and *hoxH*, are separated by a 20 bp intergenic gap (Massanz *et al.*, 1998).

3.3.3. Protein Structure

The hydrogenase moiety of SH is a heterodimer with the large (HoxH) and small subunits (HoxY) having an average mass of 52 kDa and 23 kDa respectively. Amino acid sequence alignment of HoxH has revealed highly conserved cysteine amino acids at the carboxy and amino terminal regions. The conserved cysteine amino acids of HoxH aligned with the cysteines responsible for the coordination of Ni in the large subunit of *D. gigas* Ni-Fe H_2ase. The amino acid sequence alignment of HoxY also revealed nine cysteine residues with four of the cysteine residues being highly conserved to the small subunit of the large subunit of *D. gigas* Ni-Fe H_2ase that coordinates Fe-S centers responsible for electron transfer between H_2ase dimmers. However, the amino acid sequence for HoxY is truncated by 30 % and is missing part of the protein that holds the Fe-S centers as seen in small subunit of *D. gigas* [Ni-Fe] H_2ase. Therefore, it is proposed that HoxY of the SH only possesses one [4Fe-4S] centre rather than two [4Fe-4S] that is typical of [Ni-Fe] H_2ase (Tran-

Betcke *et al.*, 1990). In addition, the truncation of HoxY may expose a part of the hydrophobic surface of the HoxH large subunit, enhancing hydrophobic interaction between the diaphorase subunit HoxU and the hydrogenase moiety. More recently, it has been proposed that a FMN group (FMN-a) is present in replacement of the second [4Fe-4S] of HoxY. This additional FMN in the small subunit HoxY is unique to the *W. eutropha* SH. The FMN-a is closely coordinated with the NiFe active site and aids the transfer of electron to the diaphorase moiety (Van der Linden *et al.*, 2004a).

The diaphorase moiety of SH is a heterodimer with the large and small subunits having an average mass of 67 and 26 kDa respectively (Tran-Betcke *et al.*, 1990). Little is known about the structure of the diaphorase moiety. However, some structural information has been derived from predicted primary amino acid structure generated from nucleotide acid sequence data and fluorescence spectral analyses (Tran-Betcke *et al.*, 1990; Van der Linden *et al.*, 2004a). The small subunit is thought to contain two [4Fe-4S] centers and has sequence similarity to the NADH: oxidoreductase dimmer of *Nitella opaca.* The large subunit is predicted to contain two [2Fe-2S] and one FMN based on sequence similarities to putative flavin-binding sites. The FMN may be required as a terminal electron donor because it can accept two reducing equivalents at a time. In contrast, the Fe-S clusters are one-electron redox groups and would require two such clusters in the small subunit (Tran-Betcke *et al.*, 1990). However, more recently it was determined that the small unit contains one [2Fe-2S] centre and one [4Fe-4S] centre, and the large subunit contains one [4Fe-4S] centre and a single FMN group (Van der Linden *et al.*, 2004a).

3.3.4. Catalytic site

The NiFe site of the SH of *W. eutropha* is unique amongst Ni-Fe hydrogenases as the SH is (1) catalytically active in the presence of O_2 and CO_2, and (2) is rapidly activated by NADH and minimally by H_2. In the model, the bimetallic Ni-Fe catalytic site the Ni is coordinated by two pairs of cysteines with the Fe sharing one cysteine pair and is coordinated by a single CO and two CN^- diatomic nonprotein ligands, resulting in an overall structure of $(Cys)_2Ni(\mu\text{-}Cys)_2Fe(CN)_2(CO)$ (Vignais *et al.*, 2001). In the SH however, only two of the four conserved cysteine coordinate with the Ni atom to provide ligands. Alternatively, a pair of remote cysteines form sulfonates coordinated with the Ni atom of SH of *W. eutropha*, with their oxygen atoms bound to nickel (Van der Linden *et al.*, 2004a). Contrary to standard H_2ases, the Ni atom of SH is also coordinated by a single CN^- and peroxide group (^-OOH). The Fe group shares one cysteine pair with the Ni group and is also coordinated by three CN^- and one CO. Giving the SH of *W. eutropha* and overall non-standard $(CN)Ni\text{-}Fe(CN)_3(CO)$ site and due to the near octahedral geometry of the coordinating groups, the SH is resistant to inactivation by either O_2 or CO as there are no available positions for these molecules to bind with the Ni group (Burgdorf *et al.*, 2005).

Rapid activation of the oxidized SH is initiated by a reductive environment of superstoichiometric NADH or substoichiometeric NADH in the presence of H_2. Under these conditions, a ^-OOH ligand is reduced to peroxide, creating a vacant coordination site on the Ni group. The release of peroxide allows H_2 molecules to gain access and bind with the vacant Ni coordination site. However, when SH are

exposed to prolonged reducing environment hydrogen catalysis is also inhibited. Prolonged reduction of SH cause the two sulfenates to be reduced to thiols and become direct ligands. The creation of direct ligands creates a standard Ni site that can be further reduced to an inactive form that is not involved in hydrogen catalysis (Burgdorf *et al.*, 2005).

3.3.5. Electron transfer from the catalytic site

The addition of a second FMN moiety, FMN-a, of the truncated HoxY is also a unique structural feature amongst Ni-Fe hydrogenases. The FMN-a group is positioned close to the Ni group of the Ni-Fe catalysis site. It is proposed that the FMN-a group functions as a two-to-one converter of electrons created from the heterolytic cleavage of H_2 at the Ni-Fe centre to the Fe-S clusters in the SH. This enables the Ni atom of the Ni-Fe centre to maintain a Ni (II) state that is poised in a constant state activation and activity. However, these structural differences also affect the conformation state of SH and the rate of H_2 catalysis.

In the SH oxidized state, the FMN of diaphorase subunit HoxF (FMN-b) and the FMN of the hydrogenase subunit HoxY (FMN-a) are firmly bound. Upon reduction activation by NADH, a peroxide is released form the sixth coordinate site of the Ni group by a reduction cascade initiated at the FMN-b in the HoxFU moiety that is transferred to the FMN-a of HoxY. The reduction activation creates a conformational change such that the FMN-a can dissociate from the SH while the SH remained in an intact tetrameric form. The NADH dehydrogenase activity is not affected as the FMN-b group is firmly bound to the HoxF subunit. The reduction of artificial electron acceptors is also unaffected, presumably by the direct hydride

transfer between HoxH and the artificial electron acceptor. However, the SH will lose all H_2ase activity over time due to the loss of the FMN-a group that is loosely bound to the HoxY subunit. This loss of activity is reversible and can be regained if excess FMN is added (Van der Linden *et al.*, 2004b).

3.3.6. Assessory genes and maturation

The H_2ase metalloprotein of *W. eutropha* undergo a complex maturation process that converts the inactive hydrogenase precursor to an active catalytic enzyme requiring at least seven accessory gene products for the uptake of metal ions, assembly of metal centers, incorporation of metal centers into inactive precursor proteins, and proteolytic processing. A complete set of *hyp* genes (*hypA1B1F1CDEX*) are located within the MBH operon, and a second copy (*hypA2B2F2*) of *hyp* genes are found downstream of the SH structural genes and are constitutively expressed from a σ^{70}-dependent promoter (Jones *et al.*, 2004).

The biosynthesis of the HoxH Ni-Fe metal site is initiated by the synthesis of the diatomic ligands. The cyanide ligands of HoxH metal centre are synthesized when HypF transfers a carbamoyl phosphate to the C-terminus cysteine in an ATP-dependent exchange reaction (Paschos *et al.*, 2002). The S-carbamoyl moiety of HypE is subsequently dehydrated to a thiocyanate in an ATP-dependent reaction (Reissmann *et al.*, 2003). The cyano ligand is then transferred to Fe when HypE is complex with the HypC and the iron-sulphur protein HypD. This process has also been proposed for the biosynthesis of the CO diatomic ligand. The $Fe(CN)_2(CO)$ group is then inserted into the HoxH apo-protein by HypC (Blokesch *et al.*, 2004; Jones *et al.*, 2004). In the HypHC complex, HypC acts as a chaperone, preventing the

folding of HoxH before the addition of the nickel group through GTP-dependent action of HypB in concert with HypA (Maier *et al.*, 1995; Olsen *et al.*, 2001).

Unlike standard organisms that metabolize H_2, *R. eutropha* harbors an additional *hyp* gene, identified as *hypX*. After the incorporation of both the $Fe(CN)_2(CO)$ group and Ni group, HypX forms a complex with HoxH and delivers the final CN diatomic ligand to the Ni group that attributes to the SH insensitivity to O_2 and CO (Bleijlevens *et al.*, 2004). Finally, the endopeptidase HoxW cleaves the C-terminal peptide, triggering the folding of HoxH around the metal site and initiating the oligomerization of the hydrogenase (Bernhard *et al.*, 1996; Kortluke & Friedrich, 1992; Massanz *et al.*, 1997; Thiemermann *et al.*, 1996).

3.3.7. Regulation of H_2ase Expression

W. eutropha H16 expresses two biochemically and physiologically distinct Ni-Fe hydrogenases to metabolize H_2 as a supplemental energy source in carbon-limited environments: an energy producing membrane bound hydrogenase (MBH) and a soluble cytoplasmic NAD-dependent hydrogenase (SH). The genes of the MBH region (*hoxKGZMLOQRTV*) and the SH region (*hoxFUYHWIhypA2B2F2*) are harbored on the pGH1 mega-plasmid and are both controlled by tightly controlled σ^{54}-dependent promoters, P_{MDH} and P_{SH} respectively (Schwartz *et al.*, 1999). Due to number of accessory proteins that are required to express H_2ases, the synthesis of Ni-Fe hydrogenases must be tightly regulated and very sensitive to specific physiological cues as the expression of these proteins is a large investment of metabolic energy and resources.

The expression of the structural genes of the SH and MBH operon is mediated by growth on carbon-limited substrates (Schwartz *et al.*, 1998) and the presence of H_2 in the environment (Lenz & Friedrich, 1998). Little is known about the molecular mechanisms of the carbon-limited control SH and MBH gene expression. However, the quality carbon environment represents an essential physiological condition for the induction of SH and MBH, as it supersedes H_2-triggered transcriptional control (Schwartz *et al.*, 1998).

In contrast, H_2-triggered transcriptional control of the SH and MBH operons has been well characterized and consists of a two-component regulatory cascade. The genes of H_2 transcriptional control (*hoxABCJ*) are also located on the pGH1 mega-plasmid and are constitutively expressed from a sigma^{70} (σ) -dependent promoter (Schwartz *et al.*, 1999). The products of the *hoxABCJ* genes, the major transcriptional response factor HoxA, and the active regulatory hydrogenase (RH) participate in the two-component regulatory cascade that regulates the expression of the SH and MBH.

In the presence of hydrogen, HoxA activities a σ^{54}–dependent RNA polymerase, that transcribes the SH and the MBH from their respective σ^{54}–dependent promoters (Schwartz *et al.*, 1999). In the absence of H_2, however, the regulatory hydrogenase represses the activation of the σ^{54}–dependent RNA polymerase by transferring a phosphate group to aspartate-55 (Asp-55)of HoxA, resulting in the suppression of SH and MBH expression.

The active hydrogen-sensing RH is a complex of the *hoxBCJ* gene products. HoxBC form the double dimer $(HoxBC)_2$ that is bound to a tetramer of HoxJ, resulting in a $Hox(BC)_2J_4$ complex. The hydrogen-sensing RH is composed of the

large subunit HoxC that harbors a standard Ni-Fe active site located deep within the center of the protein. The synthesis of the Ni-Fe site requires the actions of the Hyp proteins HypA-F that are expressed at low levels by a separate σ^{70}-dependent promoter (Buhrke *et al.*, 2001). In the presence of hydrogen, the RH binds H_2 to the Ni-Fe active site of HoxC and catalyzes the heterologous splitting of the H_2 molecule into one proton and one hydride (Bernhard *et al.*, 2001). Following the splitting of H_2, a single electron is transferred from the Ni group of the active center to the Fe-S centers of HoxB. Single electrons are then transferred to an undefined two electron-accepting organic cofactor located at the carboxy terminal extension of HoxB. The C-terminal extension of HoxB also links the H_2 sensing HoxC with the N-terminal domain of HoxJ resulting in the dimeric heterodimer complex. The redox signal is passed to the amino terminal input domain of the histidine kinase HoxJ. The initial cleavage of H_2 at the Ni-Fe active site and subsequent electron transfer reduces the activity of HoxJ, preventing the transfer of a phosphate group to HoxA. This enables HoxA to activate the σ^{54}–dependent RNA polymerase and allow expression of SH and MBH from their respective σ^{54}–dependent promoters (Schwartz *et al.*, 1999).

In the absence of any physiological stimuli, HoxJ exerts negative control on transcription by transferring a phosphate group to the phosphoryl receiver Asp-55 of HoxA. The transfer of the phosphate group to HoxA prevents the activation of σ^{54}–dependent RNA polymerase repressing expression of the SH and MBH. The negative regulation of the principal regulator HoxA of *W. eutropha* represents a unique two-component regulatory system because typical signal cascades are dependent on the positive regulation of the principal regulator (Friedrich *et al.*, 2005).

Recently, *W. eutropha* H16 has been identified as a mutated strain. The HoxA of the *W. eutropha* H16 has a mutation at Asp-55. HoxJ cannot regulate HoxA by phosphorylation of the Asp-55 as in the wild type strain. As a result, the oxygen insensitive [NiFe]-hydrogenase from *W. eutropha* H16 can be expressed constitutively under aerobic carbon-limited growth conditions (Friedrich *et al.*, 2005).

Objectives

The objective of this research project is to demonstrate the production of hydrogen from the enzymatic oxidation of methanol. This concept is based on the continuous flow of electrons from the oxidation of methanol by *Bacillus methanolicus* C1 methanol dehydrogenase to the reduction of low potential redox dye benzyl viologen by the *Wautersia eutropha* soluble hydrogenase via the recycling of the coenzyme NAD. This thesis will also provide a simple and low-cost method for determining the reaction conditions and the efficacy of coupling redox enzymes for purposes of enzymatic bioconversion of organic chemical compounds into hydrogen.

Hypothesis

H^1_o: The mutant *Bacillus methanolicus* C1 methanol dehydrogenase oxidizes methanol without the presence of the activator protein.

H^2_o: The *Wautersia eutropha* soluble hydrogenase oxidizes H_2 after being purified under aerobic conditions.

H^3_o: The electron flow from the oxidation methanol by *Bacillus methanolicus* C1 methanol dehydrogenase to the *Wautersia eutropha* soluble hydrogenase can be detected by the reduction of the low potential redox dye benzyl viologen.

Chapter 4. Purification and Characterization of *Bacillus methanolicus* C1 methanol dehydrogenase

4.1 Introduction

The methanol dehydrogenase from *Bacillus methanolicus* C1 (BmMDH) is a Type III (De Vries *et al.*, 1992) nicotinoprotein alcohol dehydrogenase consisting of 10 identical subunits of M_r 43,000 each with a subunit containing one Zn^{2+} ion and one or two Mg^{2+} ions and one tightly bound NAD(H) cofactor (Hektor *et al.*, 2002). BmMDH activity is strongly stimulated *in vitro* by a M_r 50,000 activator protein from the same organism (Arfman *et al.*, 1991). The activator protein increases the turnover rate of BmMDH 40-fold (Arfman *et al.*, 1997) by changing the methanol oxidation reaction mechanism from a ping-pong mechanism to a ternary reaction mechanism (Hektor *et al.*, 2002).

The classic NAD-binding fingerprint, GXGXXG (Wierenga *et al.*, 1986), is absent in wild type BmMDH. In contrast, the NAD cofactor is bound by a conserved Type III motif A (VSXGGGSXDXK; position 91-103 in BmMDH; Hektor *et al.*, 2002). Motif A domain displays amino acid similarity with FAD-binding domains in other Type II ADH enzymes. In these cases, the FAD functions as a cofactor and remains bound during catalysis, similar to the NAD cofactor used by BmMDH (Wierenga & Drenth, 1983; De Hoop *et al.*, 1991).

The mutation of the Ser97 to Gly97 amino acid (S97G) residue of Motif A results in a BmMDH that lacks a bound NAD(H) cofactor (Hektor *et al.*, 2002). However, the S97G mutant still has affinity for NAD(H) and displays methanol oxidation activity without the presence of the M_r 50,000 activator protein. In addition, the S97G mutation results in a very high coenzyme dependent rate of reaction that is

10 times greater (V_{max} 10400 mU.mg^{-1}) than BmMDH which requires the activator protein (V_{max} 1310 mU.mg^{-1}; Hektor *et al.*, 2002).

This experiment describes the Ser97 to Gly97 mutation of BmMDH and demonstrates the methanol oxidation activity of BmMDHS97G in the absence of the activator protein as previously demonstrated by Hektor *et al.*, (2002).

4.2. Materials and Methods

Site-directed mutagenesis of mdh gene Motif A from B. methanolicus C1

Plasmid pMDH was constructed using pBS$^+$ (Stratagene) and the 2,500 bp *BamH*I digest fragment of *B. methanolicus* C1 DNA that encodes the methanol dehydrogenase encoding gene, *mdh* (De Vries *et al.*, 1992; a gift from L. Dijkhuiken). The serine to glycine mutant at amino acid 97 (S97G) of BmMDH was introduced with the "gene splicing by overlap extension" PCR method (SOEing; Figure 4.1; Dieffenbach and Dveksler, 2003). In the first PCR round, pMDH was used as the template with primers S97G-forward (5'-cgg tgg acc t**g(a)**g **a(g)**tc **c(g)**ca cga tac agc-3') and R (5'-gcc atg tat tgt gca taa gc-3') to amplify a 450 bp PCR product. The primers S97G-right (5'-gct gtc tcg t**g(c)**g g**a(c)**g **c(t)**ga ggt cca ccg-3') and MDH-forward (5'-ggt agt aag aat gac aaa ctt ttt ca-3') were used to amplify a second 250 bp PCR product, also using pMDH as a template. The primer sequences were taken from Hektor *et al.* (2002). PCR reactions contained 200 mM 2-Amino-2-(hydroxymethyl)-1,3-propanediol hydrochloride (Tris-HCl), pH 7.5, 100 mM KCl, 100 mM $(NH_4)_2SO_4$, 10 % dimethyl sulfoxide (DSMO), 1 mg/ml bovine serum albumin (BSA) and 20 mM $MgSO_4$, 200 μM each dNTP and 250 nM each primer. Pfu DNA polymerase (1 μl) was added to all PCR reactions, and the reactions were subjected to

35 cycles of denaturing at 95 °C for 30 s, annealing at 55 °C for 30 s, followed by extension at 72 °C for 60 s in a thermocycle machine (Perkin-Elmer 9600). The PCR products were separated on a 1.0 % agarose gel (Sambrook *et al.*, 1989).

In the second round of PCR, the 450 bp and the 250 bp PCR products were used as templates for PCR SOEing using the primers R and MDH-forward to generate a 700 bp PCR product with the introduced base pair changes. PCR reactions contained 200 mM Tris-HCl, pH 7.5, 100 mM KCl, 100 mM $(NH_4)_2SO_4$, 10% DSMO, 1 mg/ml BSA and 20 mM $MgSO_4$, 200 μM each dNTP and 250 nM each primer. Pfu DNA polymerase (1 μl) was added to each PCR reactions, and the reactions were subjected to 35 cycles of denaturing at 95 °C for 30 s, annealing at 55 °C for 30 s, followed by extension at 72 °C for 60 s in a thermocycle machine (Perkin-Elmer 9600). The PCR products were separated on a 1.0 % agarose gel (Sambrook *et al.*, 1989). Rapid conformation of the silent mutation introduced to the 700 bp PCR product was assessed by restriction digest using *BamH*I restriction enzyme (New England Biolab). Direct sequencing was also used to assess the introduced mutation. The resulting 700 bp product was digested with *Nsi*I (New England Biolab) and exchanged with the original *Nsi*I fragment of pMDH resulting in a plasmid containing the S97G (pMDH S97G) mutation.

Purification of recombinant B. methanolicus C1 MDH S97G

The pMDH S97G was transformed into *E. coli* DH5α host cells by electroporation, and successful transformants were identified by plating on Luria-Bertani plus ampicillin (LB amp^+) agar selection plates (Sambrook *et al.*, 1989). Overnight cultures of *E. coli* (pMDH S97G) were grown in LB liquid medium

supplemented with 20 mM $MgSO_4$ and 100 μg ml^{-1} of ampicillin in a 2 L batch culture mixed by stirring at a rate of 650 rpm and at 37 °C. Protein expression was constitutive and under control by the *mdh* promoter (De Vries *et al.*, 1992). Cells were harvested at 0.8 OD_{600} by centrifugation at 3,800 x g for 10 min at 4 °C, washed twice in 10 mM Tris-HCl (pH 8.0), 0.4 M sucrose, 150 mM KCl, and 1 mM $MgSO_4$ (Buffer 4.1).

All procedures were carried out at 4 °C unless otherwise stated. Cells were resuspended in Buffer 4.1 at a ratio of 3:1 buffer (ml) to wet weight cell (g). Cells were disrupted in the presence of 1.0 mM dithiothreitol (DTT) and 0.1 mM α-toluenesulfonyl fluoride (PMSF) by two passages through a French press operating at approximately 140 MPa. Low-speed extracts were obtained by centrifugation at 3,800 x g for 10 min at 4 °C. Cellular membrane and large particles were removed by centrifugation at 40,000 x g for 1 h at 4 °C. The cell free lysate was resuspended in 10 ml of 50 mM potassium phosphate buffer, pH 6.5, 150 mM KCl, 5 mM $MgSO_4$, and 1 mM DTT (Buffer 4.2) and then dialyzed against the same buffer for 1.5 h and applied to 25 ml of Procion Red HE-3B-agarose resin (Pharmacia), pre-equilibrated with Buffer 4.2 for 1 h at 4 °C. The proteins were partially purified by batch separation using a vacuum manifold. The Procion Red HE-3B-agarose resin was washed in a Buckner funnel with 100 ml of Buffer 4.2. The adsorbed proteins were eluted from the resin with 100 ml of 50 mM potassium phosphate buffer (pH 6.5), 300 mM KCl, 5 mM $MgSO_4$, and 1 mM DTT (Buffer 4.3) collected in 10 ml fractions.

Determination of B. methanolicus MDH S97G protein concentrations

Protein concentrations were determined with a Bio-Rad protein determination kit using bovine serum albumin as a standard following the manufacturer's instructions. Protein fractions were analyzed via 10% SDS-polyacrylamide gel electrophoresis (SDS-PAGE) and visualized with Coomassie brilliant blue G-250 colloidal stain.

Enzyme assays of B. methanolicus MDH S97G methanol oxidation

Methanol dehydrogenase activity was assayed by measuring the reduction of NAD^+ at 340 nm spectrophotometrically on 96 well micro-assay plates (Microtitier). The reaction mixture contained 50 mM Tris-HCl (pH 8.0), 5 mM $MgSO_4$, 1 mM NAD, 1 mM DTT (Hektor *et al.*, 2002). The activity assay was initiated by the addition of methanol to a final concentration of 500 mM. The specific unit of activity was defined as the reduction of 1μmol NAD per min per mg of protein (Dixon and Webb, 1965).

4.3. Results

Site-directed mutagenesis of mdh gene Motif A from B. methanolicus C1

The S97G BmMDH mutant was constructed by the PCR "SOEing" method of site-directed mutagenesis to permit methanol dehydrogenase activity in BmMDH without the actions of the activator protein. A 250 bp and 450 bp PCR product were generated in the first round of PCR. The 250 bp and 450 bp were then used as templates in the second round with the right primer (Primer R) and left primer (MDHFor) to generate a 700 bp PCR product (Figure 4.2). The base pair mutations were confirmed by restriction digest (Figure 4.3) and direct sequencing (Figure 4.4).

The 700 bp PCR product was digested with *Nsi*I and exchanged with the *Nsi*I fragment of pMDH.

Purification of recombinant B. methanolicus MDH S97G

The S97G BmMDH mutant protein was expressed in *E. coli* grown on LB + Mg^{2+}. SDS-PAGE analysis of the cell free lysate, heat-denatured cell free lysate, and the Procion Red HE-3B-agarose resin batch purified sample (PR-BmMDH) revealed a dominant band at 43 kDa. The PR-BmMDH sample was estimated to be near electrophoretic homogeneity (Figure 4.5).

4.4. Discussion

The *B. methanolicus mdh* gene was modified by site-directed mutagenesis to create a serine to glycine amino acid substitution in Motif A at position 97 of the MDH protein. This created a construct that enables the expression of BmMDH that was independent of the activator protein for full activity. The modified BmMDH was expressed in *E. coli* DH5α cells that were transformed with the pMDH S97G and cultured in LB + Mg^{2+}. SDS-PAGE analysis revealed a dominant band at 43 kDa in the cell free lysate, heat denatured cell free lysate and Procion Red HE-3B batch purified sample (Figure 4.5; Vonck, 1991). This molecular weight corresponded to the molecular weight of the BmMDH that had been previously purified to homogeneity from *B. methanolicus* C1 under aerobic conditions from cells grown in both methanol-limiting conditions (Arfman *et al.*, 1989) and from the *B. methanolicus mdh* gene over-expressed in *E. coli* (cMDH; De Vries *et al.*, 1992). BmMDH displayed methanol oxidation activity without the co-expression of soluble M_r 50,000 activator protein because the activator protein was not co-expressed from a separate

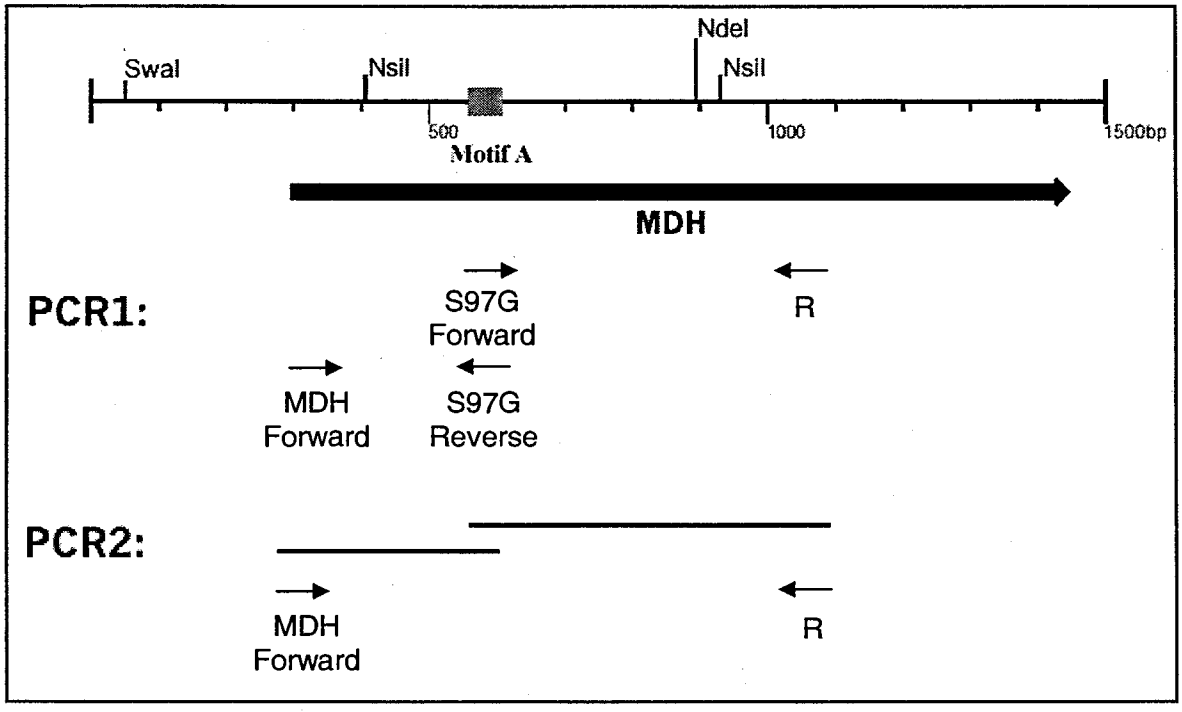

Figure 4.1: Outline of site-directed mutagenesis strategy of the MDH gene of *B. methanolicus* C1.

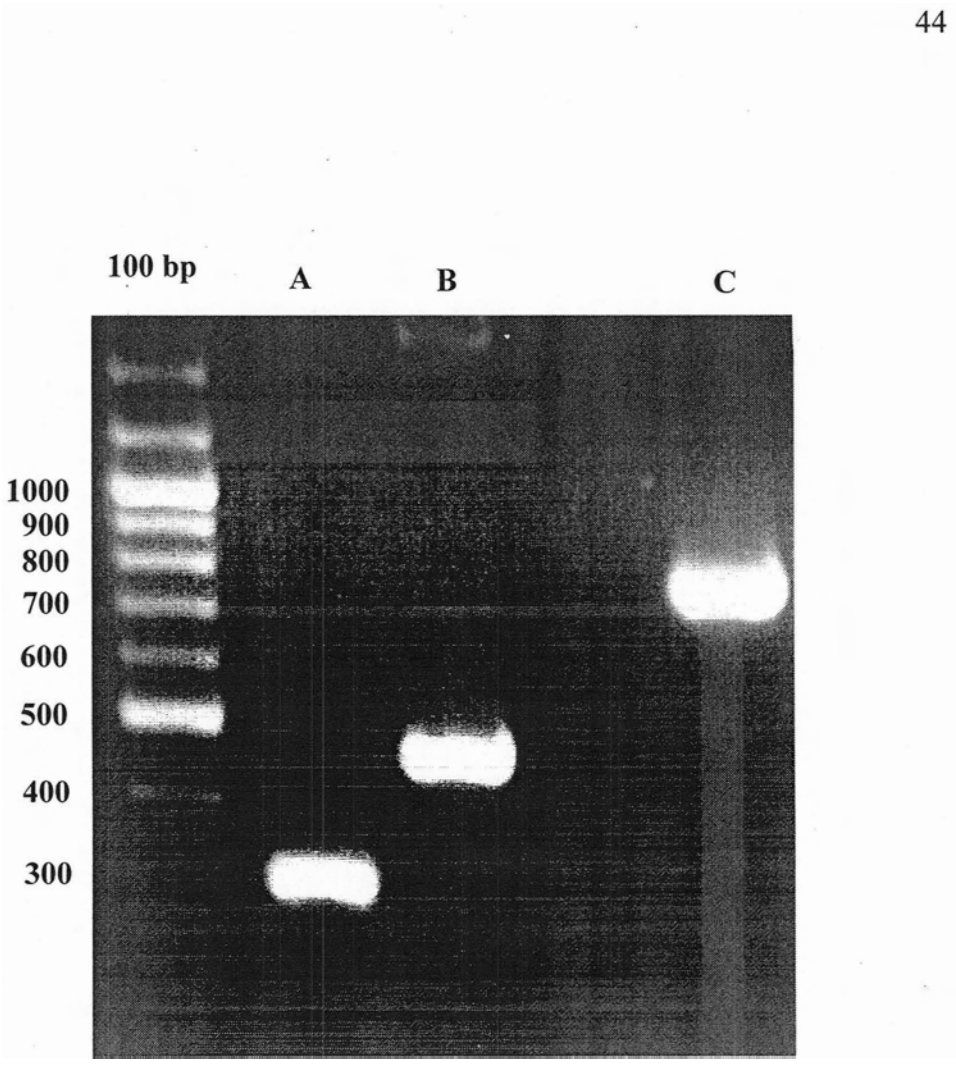

Figure 4.2: Introduction of the serine to glycine substitution at amino acid 97 of BmMDH using PCR "SOEing." (A) First round 250 bp PCR product using pMDH as a template and right primer (S97GRight: 5'-gct gtc tcg tg(c)g ga(c)g c(t)ga ggT cca ccg-3') and left primer (Primer MDHFor: 5'-ggt agt aag aat gac aaa ctt ttt ca-3'). (B) First round 450 bp PCR product using pMDH as a template and left primer (S97GLeft: 5'-cgg tgg acc t**g(a)**g **a(g)**tc **c(g)**ca cga tac agc-3') and right primer (Primer R: 5'-gcc atg tat tgt gca taa gc-3'). (C) Second round 700 bp PCR product using the 450 bp and the 250 bp PCR products as templates using right primer (Primer R: 5'-gcc atg tat tgt gca taa gc-3') and left primer (Primer MDHFor: 5'-ggt agt aag aat gac aaa ctt ttt ca-3'). A 100 bp ladder was used as a molecular size marker with sizes indicated in base pairs.

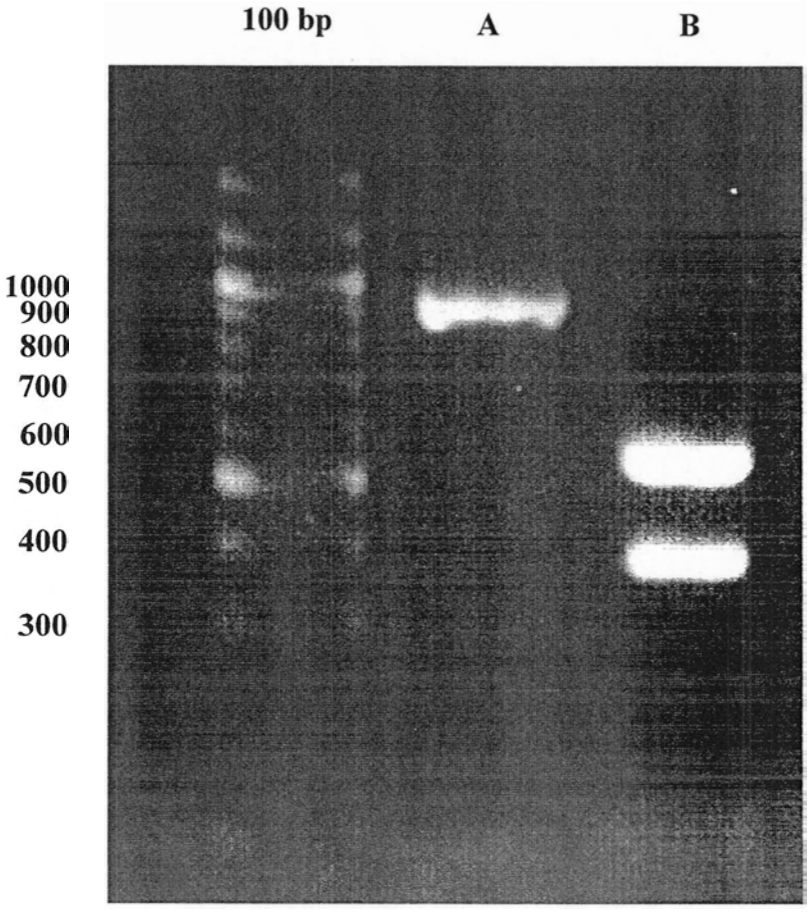

Figure 4.3: Rapid confirmation of S97G mutation by *BamHI* restriction digests of PCR "SOEing" product. (A) Uncut 900 bp PCR product using pMDHS97G as a template and M13 forward and M13 reverse primers. (B) *BamH*I restriction digest of 900 bp PCR product using pMDHS97G as a template and M13 forward and M13 reverse primers. A 100 bp ladder was used as a molecular size marker with sizes indicated in base pairs.

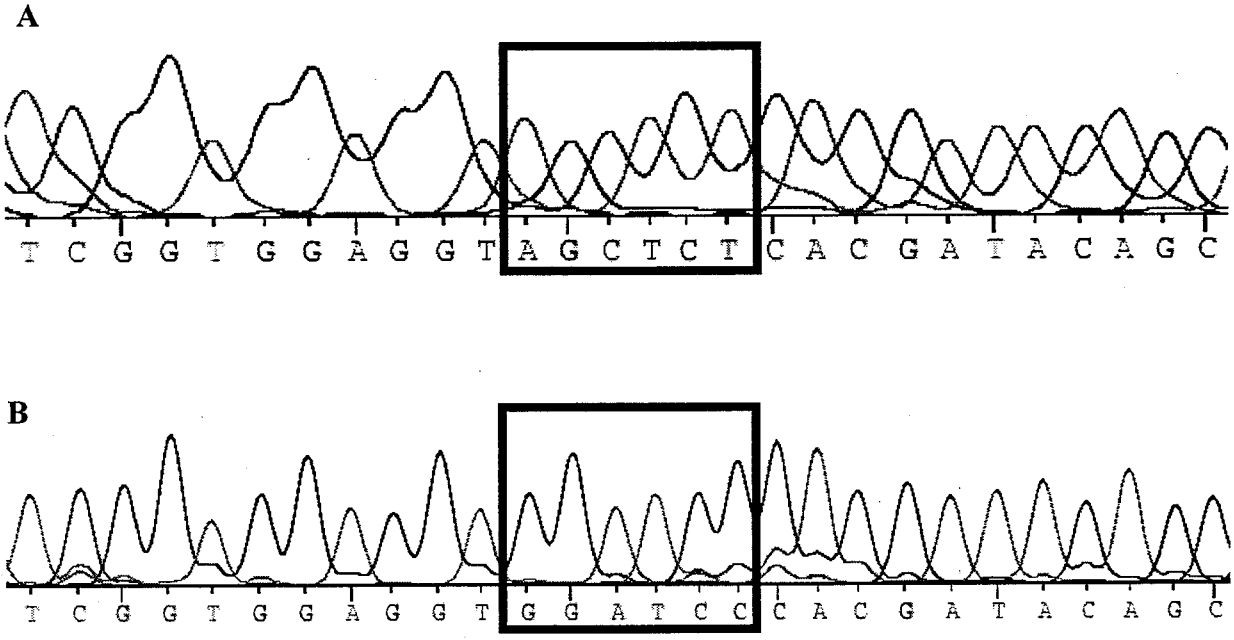

Figure 4.4: Direct sequencing of pMDH S97G. (A) Sequence of wild type pMDH. (B) Sequence of pMDHS97G mutant with introduced *BamH*I restriction site created for rapid screening.

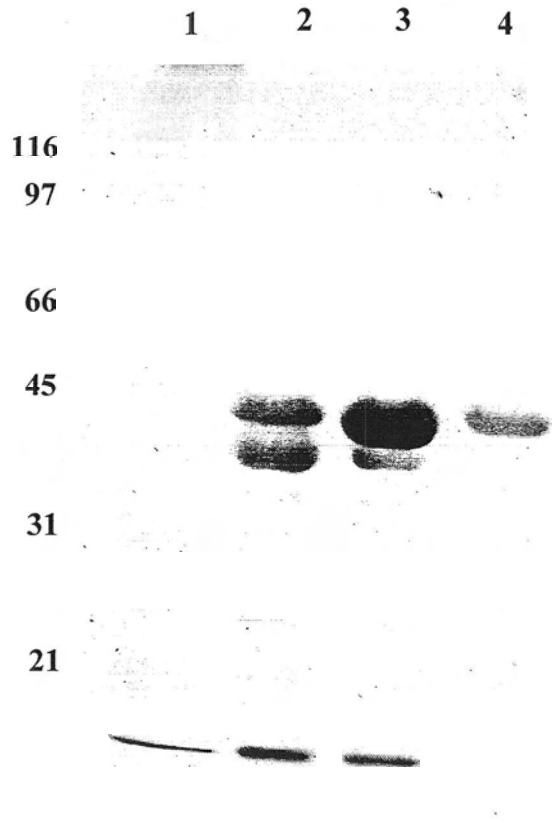

Figure 4.5: Purification of mutant BmMDH S97G protein expressed in *E. coli* grown on LB + Mg^{2+}. Proteins were separated on a 10% polyacrylamide gel by SDS-PAGE and stained with Coomassie brilliant blue G-250 colloidal stain. (1) Bio-Rad wide-range protein standard marker (15 µl), (2) cell free lysate (60 µg), (3) heat-denatured cell free lysate (60 µg), (4) Procion Red HE-3B-agarose resin batch purified sample (60µg).

Table 4.1: Purification of *B. methanolicus* C1 MDH S97G mutant extracted from *E. coli* DH 5α cultured in LB liquid media at 37 °C.

Sample	*Protein* mg	*Specific activity* milliunits/ mg	*Total activity* milliunits	*Yield* %	*Purification* fold
Cell lysate	2043.5	122.0	207.6	100	1.0
Cell free lysate	1378.8	493.0	679.7	67.5	4.0
Heat denatured cell free lysate	815.0	894.7	729.2	39.9	7.3

expression construct nor was the activator protein a native protein of *E. coli* DH5α (Table 4.1).

In wild type BmMDH, the hydrogen bond between the hydroxy group of Ser97 and the 2'-phosphate group of the NAD(H) cofactor creates a tight bond between the cofactor and the apo-enzyme. In the Ser97 to Gly97 mutant (S97G), the hydrogen bond is lost, and the NAD(H) cofactor is no longer bound to the apo-protein (Hektor *et al.*, 2002). Although, the apo-protein cannot tightly bind the NAD(H) coenzyme, the NAD(H)-cofactor site of the S97G mutant can still function as a NAD(H)-coenzyme site. Therefore, the Ser97 to Gly97 mutation changes the wild type BmMDH from a ping-pong to a coenzyme-dependent ternary complex mechanism. This results in a mutant protein that is not only independent of the activator protein but exhibits a V_{max} for methanol oxidation that is 10 times higher (10400 $mU.mg^{-1}$) than the wild type protein (1310 $mU.mg^{-1}$; Hektor *et al.*, 2002).

A maximum specific activity of the recombinant BmMDH S97G expressed in E. coli was 894.7 $nmol.min^{-1}.mg^{-1}$, observed with the heat denatured cell free lysate protein extract (Table 4.1). The BmMDH S97G specific methanol dehydrogenase activity determined in this study was lower than the reported methanol dehydrogenase V_{max} (1000-1200 $nmol.min^{-1}.mg^{-1}$) for wild type BmMDH extracted from *Bacillus methanolicus sp.* C1 cytoplasmic extracts cultured under methanol-limiting conditions in the presence of Mg^{2+} grown at 50 °C and pH 9.5 (Arfman *et al.*, 1989). However, measures of enzyme activity determined by velocity maxima cannot be compared with enzyme activity determined by specific activity. This is because velocity maxima represent a theoretical limit of enzyme activity at an infinite

substrate concentration, while specific activities represent an actual rate of activity at a defined substrate concentration (Dixon & Webb, 1965).

The heat denaturing of the cell free lysate proved to be an efficient method of protein fractionation that had not been previously used to purify BmMDH. Heat denaturing allowed for the separation of proteins based on their thermostability. The wild type BmMDH protein is thermostable, because the protein is naturally expressed in *B. methanolicus* C1 during optimum growth temperature at 50 °C. In contrast, the majority of proteins expressed in *E. coli* are heat liable, because *E. coli* optimum growth temperature is around 37 °C. Heat denaturing of the cell free lysate resulted in the denaturing and aggregation of the *E. coli* heat liable protein that was subsequently removed by centrifugation. During the heat denaturing procedure, the expressed thermostable BmMDH S97G was unaffected and remained soluble and active. SDS-PAGE analysis of the heat denaturing of *E. coli* cell free lysate containing expressed BmMDH S97G mutant protein revealed a dominant band at 43 kDa corresponding to the molecular weight of BmMDH monomer (Vonck *et al.*, 1991). The heat denaturing procedure also resulted in a 7.3 fold purification and 39.9 % recovery of BmMDH (Table 4.1). This single step also resulted in an increase in specific activity that was higher than the reported specific activity of the wild type BmMDH after three column purification steps.

The batch protein purification using Procion Red HE-3B resin also proved to be an efficient method of purifying BmMDH. Traditionally, BmMDH has been purified in three chromatography steps resulting in a large loss of protein yield (Hektor *et al.*, 2002). Affinity chromatography has advantages over other

chromatography techniques in the case of enzymes with high specificity and a large capacity for the ligand-resin support. If these two conditions are met, the purification of enzymes can be carried out in one chromatography step with high purity and little loss in protein yield. Dye ligands have been used to purify enzymes that require NAD(P)(H) as a co-enzyme (Price & Stevens, 1989). SDS-PAGE analysis of the Procion Red HE-3B purified BmMDH S97G sample revealed a dominant band at 43 kDa (Figure 4.7), corresponding to the molecular weight of BmMDH monomer (Vonck *et al.*, 1991). In addition, the Procion Red HE-3B purified BmMDH S97G sample also displayed enzyme activity towards methanol.

Although the Procion Red HE-3B purified BmMDH S97G sample also displayed enzyme activity towards methanol activity was readily lost even in the presence of 10 % glucose or 10 % glycerol when kept at 4 ^{o}C. The loss of activity was not likely to be the result of dilution effects seen in wild type BmMDH that is correlated with the activity of the activator protein (Arfman *et al.*, 1989) because the BmMDH S97G did not require the activator protein for full activity. As well, enzyme activity can be detected immediately after batch purification. However, methanol dehydrogenase activity was gradually lost over time. This loss of activity was probably due to a loss in protein structural stability as a result of water effects promoted by the dilute concentration of the BmMDH S97G obtained after the chromatography purification.

Although the primary (and usually secondary) structure of proteins is quite stable, the tertiary structure can be disrupted quite easily. Proteins are the most stable when conditions mimic the in vivo environment, such as high protein concentrations.

Often, the chromatography techniques used to isolate proteins result in a dilution in protein concentration. As a result, the activity of enzymes may be lost due to disruption of the tertiary structure during protein purification. To avoid losses in enzyme activity, the addition of a second inert protein, such as BSA, will increase protein concentrations of dilute samples and prevent the loss of enzyme activity as a result of proteins "sticking" to glass and plastic surfaces. However, the addition of a second protein does contaminate the sample, and the additional protein may have to be removed in later protein purification steps. Alternatively, concentrating the protein sample through dialysis or ultrafiltration can preserve the activity of enzyme. However, the enzyme activity may be lost due to changes in the solution conditions during the dialysis procedure. In contrast, ultrafiltration leads to the concentration of an enzyme solution without changing the solution conditions, therefore, preserving enzyme activity.

Although this experiment did not result in a stable isolated BmMDH S97G protein, oxidation activity towards methanol without the presence of the activator protein was observed.

Chapter 5. Purification and characterization of *Wautersia eutropha* H16 hydrogen dehydrogenase

5.1. Introduction

The soluble hydrogenase (SH) of *W. eutropha* is a NAD^+-dependent [NiFe]-H_2ase unique among [NiFe]-H_2ases. Its novelty is that the SH can be isolated under aerobic conditions in a stable oxidized non-active state and can regain activity by the presence of NADH and H_2 (Schneider & Schlegel, 1976).

The SH is a heterodimer consisting of a hydrogenase and a diaphorase moiety. The hydrogenase moiety of SH is composed of a large 52 kDa subunit (HoxH) that harbors the [NiFe] catalytic site and small 23 kDa subunit (HoxY) that contains [Fe-S] centers necessary for the electrical communication between the hydrogenase and diaphorase moiety. The diaphorase moiety is composed of a large 67 kDa (HoxF) subunit that contains the terminal FMN electron donor/acceptor that interacts with exogenous redox partners and a small 26 kDa (HoxU) subunit that contains both Fe-S centers and FMN for the electrical communication between the hydrogenase and diaphorase moiety (Schneider & Schlegel, 1976; Tran-Betcke *et al.*, 1990; Van der Linden *et al.*, 2004b).

The genes required for the expression of the SH are harbored within the MBH and the SH operons of the *W. eutropha* pGH1 mega-plasmid. In addition, both operons possess σ^{54}-dependent promoters (Schwartz *et al.*, 1999). The expression of the SH is controlled by a unique two-component regulatory system that involves the principal regulator HoxA and a hydrogen-sensing regulatory hydrogenase (RH). The HoxA negatively regulates expression of the SH by activating a σ^{54}–dependent RNA polymerase that transcribes the SH genes from the σ^{54}–dependent promoters of the

SH operon (Schwartz *et al.*, 1999). The principle regulator, HoxA, is in turn positively regulated by the RH. In the absence of hydrogen, the RH phosphorylates the HoxA, thereby preventing HoxA from completing with the σ^{54}–dependent RNA polymerase and preventing transcription of the SH genes from the σ^{54}–dependent promoters of the SH operon. In the presence of hydrogen, the HoxA is not phosphorylated; therefore HoxA can complex with the σ^{54}–dependent RNA polymerase promoting the transcription of the SH genes resulting in expression of the SH (Friedrich *et al.*, 2004).

Wild type *W. eutropha* SH has been expressed in heterotrophic cultures grown on mineral salt media supplemented with carbon-limited substrates (Schneider & Schlegel, 1976) under an atmosphere of H_2 (Lenz & Friedrich, 1998). However, the requirement to use an H_2 atmosphere for the induction of the SH expression from the wild type *W. eutropha* presents several technical drawbacks for laboratories that are not equipped for large-scale anaerobic culturing experiments. In addition, there are several safety issues involved, because H_2 gas is potentially explosive (Schlegel *et al.*, 1961).

Recently, *W. eutropha* H16 has been identified as a mutated strain. The HoxA of the *W. eutropha* H16 has a mutation at Asp-55. HoxJ cannot regulate HoxA by phosphorylation of the Asp-55 as in the wild type strain. As a result, the structural genes of the SH operon are constitutively transcribed by the HoxA activated σ^{54}–dependent RNA polymerase, under carbon-limited growth conditions (Friedrich *et al.*, 2005).

This experiment describes the protein purification of SH from *W. eutropha* H16 cultured under aerobic carbon-limited conditions and demonstrates the activity of SH towards H_2 oxidation.

5.2. Materials and Methods

Culturing of Wautersia eutropha H16

Wautersia eutropha strain H16 (German Collection of Microorganisms and Cell Cultures: DSMZ 428) was grown in 1 L of mineral salts medium containing: KH_2PO_4 (1.5 g), $Na_2HPO_4.12\ H_2O$ (9.0 g), NH_4Cl (0.2 g), $MgSO_4.7\ H_2O$ (0.2 g), $CaCl_2.2H_2O$ (0.01 g), $FeCl_3.6\ H_2O$ (5×10^{-3} g), $NiCl_2.6\ H_2O$ (2×10^{-5} g) adjusted to pH 7.0. Cells were cultivated in 1 L heterotrophic batch cultures in mineral media supplemented with 0.4 % (wt/vol) fructose (FN) at room temperature with aeration and stirring until a 0.8 OD_{600} was achieved after approximately 48 to 72 h. An aliquot of *W. eutropha* cultured in FN was used to inoculate (0.1 %) four batch cultures (4 L each) of mineral media supplemented with 0.2 % (wt/vol) fructose and 0.2 % (vol/vol) glycerol (FGN) and was cultured at room temperature with aeration and stirring until an 0.8 OD_{600} was achieved after approximately 48 to 72 h (Schneider & Schlegel, 1976).

Protein purification of W. eutropha H16 soluble hydrogenase

W. eutropha cultured heterotrophically in FGN minimal mineral media were harvested by centrifugation at 3,800 x g for 10 min at 4 °C, washed twice in 50 mM Tris-HCl (pH 7.0), 5 mM $MgSO_4$, and 0.5 mM $NiCl_2$ (Buffer 5.1). Cells were resuspended in buffer A at a ratio of 3:1 buffer (mL) to wet weight cell (g). Cells were disrupted in the presence of 0.5 mM ferricyanide and 0.1 mM PMSF by two

passages through a French press operating at approximately 140 MPa. Low-speed extracts were obtained by centrifugation at 3,800 x g for 10 min at 4 °C. Cellular membrane and large particles were removed by centrifugation at 100,000 x g for 1 h at 4 °C (Schneider & Schlegel, 1976).

All procedures were carried out at 4 °C unless otherwise stated. The low-speed extract was diluted to 20-25 mg protein/ml, and N-cetyltrimethylammonium bromide (CTAB) was added to a final ratio of 1 mg CTAB per 1 mg of protein. The precipitate was removed by centrifugation at 10,000 x g for 10 min. The supernatant from the CTAB treatment was further purified by the addition of solid ammonium sulfate to give a 40 % saturated solution. The precipitate was removed by centrifugation at 10,000 x g for 10 min. The supernatant was then brought to a final concentration of 60 % saturation with solid ammonium sulfate, and the precipitant was collected by centrifugation at 10,000 x g for 10 min (Schneider & Schlegel, 1976). The pellet was dissolved in 10 ml of 50 mM potassium phosphate buffer (pH 6.2, 200 mM KCl, 5 mM $MgSO_4$, and 0.5 mM $NiCl_2$ (Buffer 5.2) and then dialyzed against the same buffer for 1.5 hr. Hydrogenase was purified by batch separation using a vacuum manifold. The dialyzed sample was then applied to 25 ml of Procion Red HE-3B-agarose resin (Pharmacia), pre-equilibrated with Buffer 5.2 for 1 hr at 4 °C. Procion Red HE-3B-agarose resin was washed in a Buckner funnel with 100 ml of Buffer 5.2. The adsorbed protein was eluted off the resin with 100 ml of 50 mM potassium phosphate buffer (pH 6.2), 500 mM KCl, 5 mM $MgSO_4$, and 0.5 mM $NiCl_2$ (Buffer 5.3) collected in 10 ml fractions

Protein Determination of Wautersia eutropha soluble H_2ase

Protein concentrations were determined with a Bio-Rad protein determination kit using bovine serum albumin as a standard, following the manufacturer's instructions. Protein fractions were analyzed via 10% SDS-polyacrylamide gel electrophoresis (SDS-PAGE) and visualized with Coomassie brilliant blue G-250 colloidal stain.

Enzyme assays

Hydrogenase activity was assayed by measuring the reduction of NAD at 340 nm spectrophotometrically on 96 well micro-assay plates (Microtitier). The reaction mixture contained H_2 saturated 50 mM Tris-HCl (pH 8.0), 5 mM $MgSO_4$, 0.5 mM $NiCl_2$, 0.001 mM NADH (Schneider & Schlegel, 1976). The activity assay was initiated by the addition of NAD to a final concentration of 0.8 mM (Schneider & Schlegel, 1976). The specific unit of activity was defined as the reduction of 1 μmol NAD per min per mg of protein (Dixon & Webb, 1965).

5.3. Results

Expression and purification of H_2ase from W. eutropha H16

W. eutropha H_2ase was expressed in heterotrophic batch cultures grown on mineral salt medium with fructose followed by mineral salt medium with fructose plus glycerol, as described by Schneider and Schlegel (1976). SDS-PAGE analysis of the ammonium sulfate precipitated *W. eutropha* cell lysate sample revealed three strong bands at 52, 26, and 23 kDa, and faint bands at 52, 26, and 23 kDa were also seen in the cell lysate and Procion Red HE-3B-agarose resin batch purified (PR-H_2ase) sample (Figure 5.1.; CTAB purification data not shown).

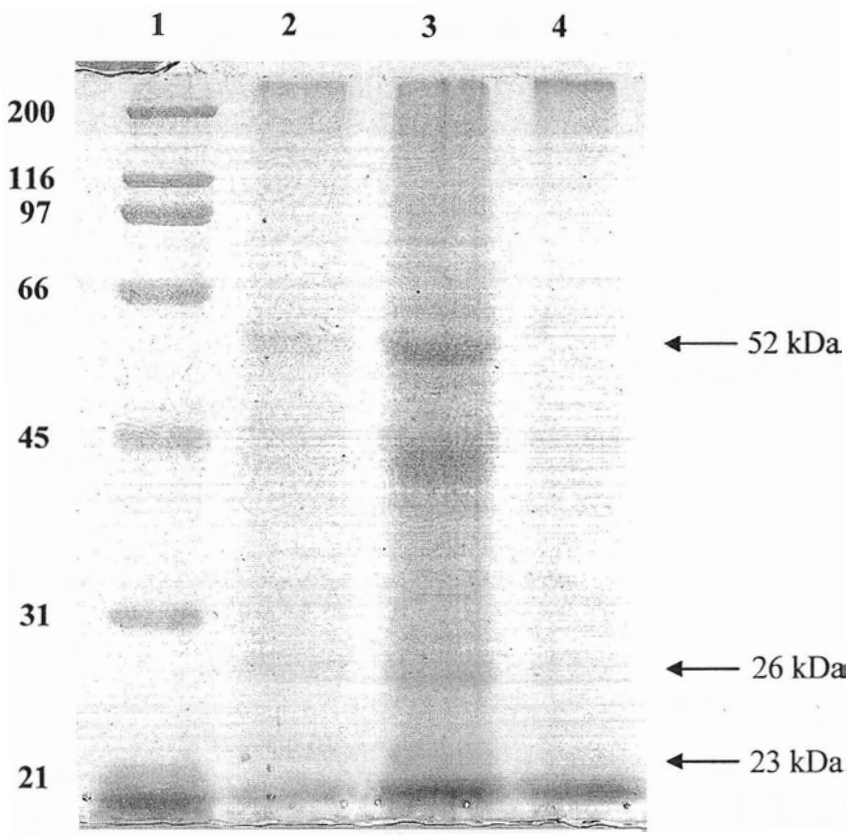

Figure 5.1: Purification of SH protein expressed in *W. eutropha* cultured in FN and FGN minimal mineral media under heterotrophic growth conditions. Proteins were separated on a 10 % polyacrylamide gel by SDS-PAGE and stained with Coomassie brilliant blue G-250 colloidal stain. (1) Bio-Rad wide-range protein standard marker (kDa), (2) cell free lysate, (3) 40 %-60 % ammonium sulfate precipitation, and (4) Procion Red HE-3B-agarose resin batch purified sample.

Table 3.1: Purification of H_2ase protein expressed in *W. eutropha* cultured in FN and FGN minimal mineral media under heterotrophic growth conditions.

Sample	Protein	Specific activity	Total activity	Yield	Purification
	mg	*milliunits/ mg*	*milliunits*	*%*	*fold*
Cell free lysate	568.75	865.7	492.4	100.0	1.0
CTAB precipitation	232.92	4087.6	952.1	41.0	4.7

Enzyme assays

The *W. eutropha* cell lysate, CTAB precipitation, ammonium sulfate precipitation and PR-H_2ase sample hydrogen dehydrogenase activity (Table 5.1). However, the PR sample readily lost enzyme activity even in the presence of 10 % glucose or 10 % glycerol when kept at 4 °C.

5.4. Discussion

The *W. eutropha* H16 mutant strain was successfully cultured under carbon-limited growth conditions. SDS-PAGE analysis of the ammonium sulfate (AS) precipitated *W. eutropha* H16 cell lysate sample revealed three strong bands at 52, 26, and 23 kDa. Faint bands at bands at 52, 26, and 23 kDa were also seen in the cell lysate and Procion Red HE-3B-agarose resin batch purified (PR-H_2ase) samples. The 52 kDa and the 23 kDa molecular weight bands from the SDS-PAGE analysis of the cell lysate, AS, and the PR-H_2ase sample correspond to the proposed heterodimer hydrogenase moiety of the SH, with the large (HoxH) and small subunits (HoxY) having an average mass of 52 kDa and 23 kDa respectively (Schneider & Schlegel, 1976; Tran-Betcke, 1990; Van der Linden *et al.*, 2004b).

The 26 kDa molecular weight bands from the SDS-PAGE analysis of the SH cell lysate, AS, and the PR-H_2ase sample correspond to the small subunit of the proposed heterodimer diaphorase moiety of the SH. However, the presence of the 67 kDa large subunit of the diaphorase moiety is not visualized by SDS-PAGE analysis in the SH cell lysate, AS, or the PR-H_2ase sample (Schneider & Schlegel, 1976; Tran-Betcke *et al.*, 1990; Van der Linden *et al.*, 2004b).

The oxidized SH purified in this study only became active when NADH is present in the assay buffer (data not shown). Rapid activation of the oxidized SH is initiated by a reductive environment of superstoichiometric NADH or substoichiometeric NADH in the presence of H_2. Under these conditions, a –OOH ligand is reduced to peroxide, creating a vacant coordination site on the Ni group. The release of peroxide allows H_2 molecules to gain access and bind with the vacant Ni coordination site (Burgdorf *et al.*, 2005)

The CTAB, AS, and PR-H_2ase purification steps provided limited purification of the SH (Figure 5.1). Numerous bands were seen in all sample preparation. These bands are in addition to the bands corresponding to the large (HoxH) and small subunits (HoxY) of the hydrogenase and the small subunit (HoxU) of diaphorase of the SH. In addition, a band at 67 kDa that would correspond to the large subunit (Hox F) of the diaphorase was absent.

The purification of proteins by batch separation does have advantages: (1) less time is required to perform the purification, (2) large amounts of lysate can be processed, and (3) clearing the lysate prior to purification is generally not required. However, the isolation of a single protein using batch separation is only possible if the expression rate of the protein is relatively high. In contrast, the batch separation procedure is not an ideal protein separation technique if protein expression is relatively low. When protein concentrations are low, the result is a mixture of the protein: a small quantity of the protein of interest and many unwanted proteins. In these situations, column purification is the preferred method for protein isolation

because this method has the potential to separate a mixture of proteins into individual components.

The SH has been previously purified in two chromatography steps using Procion Red HE-3B (Schneider *et al.*, 1983). However, the procedure differed from this study in three major ways. Firstly, the *W. eutropha* was grown in a 14 L lithoautotrophic culture under an atmosphere of H_2. Large cultures are required for the purification of the SH because the expression of the SH under these conditions only comprises approximately 2.0% of total cytosolic protein. Secondly, the SH was eluted during affinity Procion Red HE-3B column chromatography using linear gradients. Elution of protein by linear gradient would allow for greater separation of the SH from other unwanted cytosolic proteins. In this study, the proteins were eluted from the Procion Red HE-3B matrix by batch separation. Thirdly, the purification of SH by Procion Red HE-3B affinity chromatography was followed by ion exchange chromatography. This second chromatography step would further separate the SH from other unwanted cytosolic proteins of *W. eutropha* H16, resulting in a more purified SH sample.

Although this experiment did not result in a single isolated SH protein, oxidation activity towards H_2 was observed in partially purified protein from *W. eutropha* H16 cultures grown under aerobic carbon-limited conditions.

Chapter 6. Coupled enzyme oxidation of methanol

6.1. Introduction

The chemical conversion of organic compounds using traditional synthetic methods predominantly uses toxic metals and expensive complex chemicals (Kroutil *et al.*, 2004; Nunez *et al.*, 1999; Kato *et al.*, 1973). In contrast, the use of biological catalysts for the chemical conversion of organic compounds offers an environmentally friendly and renewable alternative (Kroutil *et al.*, 2004).

Enzymes have been used to catalyze the chemical conversion of several organic compounds (Kato *et al.*, 1973; Kroutil *et al.*, 2004; Nunez *et al.*, 1999). A common chemical conversion strategy is to oxidize alcohol using redox enzymes requiring nicotinamide cofactors, such as NADH and NADPH. The two strategies for the chemical conversion of alcohols are coupled-substrate and coupled-enzyme.

The coupled-substrate system is the simplest system as it employs only one dehydrogenase enzyme. In the coupled-substrate system, the recycling of cofactor is driven by oxidation and reduction of two substrates. However, the coupled-substrate system requires an excess of one of the substrates to drive the equilibrium in the direction of the desired product. Therefore, the rate of production is eventually impeded by cosubstrate inhibition. Alternatively, the coupled-enzyme approach utilizes two enzymes for the recycling of the cofactor. The coupled-enzyme approach, therefore, does not suffer the limitation of cosubstrate inhibition and consequently the yield of the desired product is much higher (Kroutil *et al.*, 2004; Nunez *et al.*, 1999).

Woodward *et al.* (2000) successfully demonstrated the biological conversion of glucose to hydrogen. However, glucose is not an efficient hydrogen carrier due to its low hydrogen to carbon ratio. Methanol is a better substrate than glucose because methanol has a higher hydrogen to carbon ratio. In addition, methanol is liquid at room temperature, making methanol compatible with the existing fossil fuel distribution and storage infrastructure.

Spectrophotometric methods using low-potential redox dyes to monitor the electron flow during hydrogen production by hydrogenase enzymes is a routine procedure. Low-potential redox dye compounds, such as benzyl viologen (BV), change color upon being reduced by the hydrogenase. This change in color is then used to infer the production of hydrogen. Therefore, it is theoretically possible to monitor the bioconversion of methanol to hydrogen using spectrophotometric methods.

This experiment will describe the coupled-enzyme production of hydrogen using the BmMDH S97G and SH by monitoring the electron flow that results in the reduction of the redox mediator benzyl viologen dichloride.

6.2. Methods

Preparation of recombinant MDH S97G crude protein extraction

Overnight cultures of *E. coli* harboring the pMDH S97G were grown in LB medium supplemented with 20 mM MgSO4 and 100 μg ml^{-1} of ampicillin in a 2 L batch culture with a stir rate of 650 rpm, with aeration, and at 37 °C. Protein expression was constitutive and under control by the promoter of the *mdh* gene (De Vries *et al.*, 1992). Cells were harvested at 0.8 OD_{600} by centrifugation at 3,800 x g

for 10 min at 4 °C, washed twice in 10 mM Tris-HCl (pH 8.0), 1 mM DTT, and 5 mM $MgSO_4$ (Buffer 6.1).

All procedures were carried out at 4 °C unless otherwise stated. *E. coli* cells were resuspended in Buffer 6.1 at a ratio of 3:1 buffer (ml) to wet weight cell (g). Cells were disrupted in the presence of 1.0 mM DTT and 0.1 mM PMSF by two passages through a French press operating at approximately 140 MPa. Low-speed extracts were obtained by centrifugation at 3,800 x g for 10 min. Cellular membrane and large particles were removed by centrifugation at 40,000 x g for 1 h. The cell free lysate was heat denatured for 50 min at 55 °C then incubated on ice for 15 min. Precipitated proteins were removed by centrifugation at 10,000 x g for 20 min. The heat denatured cell free lysate was further purified by the addition of solid ammonium sulfate to give a 30 % saturated solution. The precipitate was removed by centrifugation at 10,000 x g for 10 min. The supernatant was then brought to a final concentration of 45 % saturation with solid ammonium sulfate, and the precipitant was collected by centrifugation at 10,000 x g for 10 min, and the supernatant was discarded. The pellet was dissolved in Buffer 6.1.

Preparation of W. eutropha H16 soluble H_2ase crude extract

Wautersia eutropha strain H16 (ATCC 17699, DSM 428) was grown in 1 L of mineral salts medium containing: KH_2PO_4 (1.5 g), $Na_2HPO_4.12\ H_2O$ (9.0 g), NH_4Cl (0.2 g), $MgSO_4.7\ H_2O$ (0.2 g), $CaCl_2.2H_2O$ (0.01 g), $FeCl_3.6\ H_2O$ (5×10^{-3} g), $NiCl_2.6\ H_2O$ (2×10^{-5} g) adjusted to pH 7.0. Cells were cultivated in 1 L heterotrophic batch cultures in mineral media supplemented with 0.4 % (wt/vol) fructose (FN) at room temperature with aeration and a stir rate of 650 rpm until a 0.8 OD_{600} was achieved

after approximately 48 to 72 h. An aliquot of *W. eutropha* cultured in FN was used to inoculate (0.1 %) four batch cultures (4 L each) of mineral media supplemented with 0.2 % (wt/vol) fructose and 0.2 % (vol/vol) glycerol (FGN). The FGN culture was incubated at room temperature with aeration and stirring at rate of 650 rpm until a 0.8 OD_{600} was achieved after approximately 48 to 72 h (Schneider & Schlegel, 1976).

W. eutropha cultured heterotrophically in FGN minimal mineral media were harvested by centrifugation at 3,800 x g for 10 min at 4 °C, washed twice in 50 mM Tris-HCl (pH 7.0), 5 mM $MgSO_4$, and 0.5 mM $NiCl_2$ (Buffer 6.2). Cells were resuspended in buffer A at a ratio of 3:1 buffer (ml) to wet weight cell (g). Cells were disrupted in the presence of 0.5 mM ferricyanide and 0.1 mM PMSF by two passages through a French press operating at approximately 140 MPa. Low-speed extracts were obtained by centrifugation at 3,800 x g for 10 min at 4 °C. Cellular membrane and large particles were removed by centrifugation at 100,000 x g for 1 h at 4 °C (Schneider & Schlegel, 1976).

All procedures were carried out at 4 °C unless otherwise stated. The cell free supernatant was fractionated by the addition of solid ammonium sulfate to give a 40 % saturated solution. The precipitate was removed by centrifugation at 10,000 x g for 10 min. The supernatant was then brought to a final concentration of 60 % saturation with solid ammonium sulfate, and the precipitant was collected by centrifugation at 10,000 x g for 10 min and the supernatant was discarded (Schneider & Schlegel, 1976). The pellet was dissolved in Buffer 6.2.

Determination of crude extract protein concentration

Protein concentrations were determined with a Bio-Rad protein determination kit using bovine serum albumin as a standard following the manufacturer's instructions.

Activity assays for B. methanolicus MDH S97G

The presence of methanol dehydrogenase activity was assayed by measuring the reduction of NAD^+ at 340 nm spectrophotometrically on 96 well micro-assay plates (Microtitier). The reaction mixture contained 50 mM Tris-HCl (pH 8.0), 5 mM $MgSO_4$, 1 mM NAD, 1 mM DTT (Hektor *et al.*, 2002), and an appropriate amount of enzyme to detect activity.

Activity assays for W. eutropha H16 soluble H_2ase

The presence of hydrogenase activity was assayed by measuring the reduction of NAD^+ at 340 nm spectrophotometrically on 96 well micro-assay plates (Microtitier). The reaction mixture contained H_2 saturated 50 mM Tris-HCl (pH 8.0), 5 mM $MgSO_4$, 0.5 mM $NiCl_2$ (Schneider & Schlegel, 1976) and an appropriate amount of enzyme to detect activity.

Activity assays for coupled enzyme oxidation methanol

Coupled enzyme activity was observed by the development of a deep blue coloration in the reaction mixture. Unless otherwise stated, all reactions were carried out under an atmosphere of nitrogen. The reaction mixture (1 mL) contained 50 mM Tris-HCl (pH 8.0), 5 mM $MgSO_4$, 1 mM DTT, 1 mM NAD^+, and 1 mM BV (Buffer 4.3). Reactions contained 100 μg of crude protein extract and were initiated by the addition of 500 mM of degassed methanol under an atmosphere of nitrogen incubated at room temperature.

6.3. Results and Discussion

The activity of hydrogenases and, therefore, the enzymatic production of hydrogen can be measured by four general methods: gas chromatography, gas pressure analysis in a manometer, amperometrically using a Clark-type electrode, and by spectrophotometry. Of the four techniques, measuring the production or oxidation of H_2 spectrophotometry using low-potential dye compounds is simplest and most cost effective technique (Cammack *et al.*, 1994). The SH is able to use a variety of redox partners including BV. In the presence of H_2, the SH will oxidize H_2 and reduce BV as a redox partner (Tran-Betcke *et al.*, 1990).

In the controls containing only the BmMDH extract, the reduction of BV by BmMDH did not occur as a color change was not observed (Table 6.1). However, side reactions resulting in BV reduction are possible as BmMDH extracts were used and not a purified sample of BmMDH (Dijkhuizen *et al.*, 1988; Arfman *et al.*, 1989). However, no color change in the reaction mixture was noted; therefore, these possible side reaction may not have resulted in a net change in BV reduction or BV reduction may not have occurred at all.

In the controls containing only the H_2ase extract, the reduction of BV was observed indicated by a slight color change (Table 6.1). The SH is normally in an inactive state when extracted under an aerobic environment. However, the reductive environment created by the presence of DTT in the reaction mixture would reductively activate the SH (Burgdorf *et al.*, 2005). Although the reaction buffer and methanol solutions were de-gassed and stored under an anaerobic atmosphere of N_2, the protein extracts were not stored under anaerobic conditions and a small amount of

Table 6.1: Coupled enzyme oxidation of methanol (M) and reduction of benzyl (BV) by BmMDH and H_2ase at room temperature under anaerobic conditions.

Reaction condition	**NAD^+ Reduction***
Controls	
BmMDH + M	+
H_2ase + H_2	+
	Color development**
B	-
B + M	-
B + BmMDH	-
B + BmMDH + M	-
B + H_2ase	+
B + H_2ase + M	+
B + BmMDH + H_2ase	+
Experimental condition	
B + BmMDH + H_2ase + M	++

*No reduction of NAD^+ (-), reduction of NAD^+ (+)
**No color development (-), faint color development (+), strong color development (++), reaction buffer (RB).

H_2 may have been present. Once activated, the SH oxidized the H_2 present in the protein extract resulting in the observed color change.

In the experimental condition containing both BmMDH and SH extracts, BV was reduced indicated by a strong color change (Table 6.1). The color change was also more pronounced as compared to SH alone, indicating a greater amount of BV was reduced. This was expected because combining both oxidation and reduction reactions of NAD(H) into one process, it is possible to continually oxidize methanol and reduce BV by recycling of the NAD^+/NADH cofactor (Nunez *et al.*, 1999). This continual cycling results in a greater utilization of the methanol substrate resulting in greater amounts of reduced BV as seen in the more dramatic color change.

Although the reduction of low potential redox dyes is a common method used to measure hydrogenase activity, this method is an indirect measure of hydrogen production and does not measure hydrogen production or oxidation directly. As well, the redox dyes have a lower redox potential than that of H_2. Therefore, the rate of redox dye reduction may not reflect the rate of hydrogen production, if hydrogen production occurs at all (Huang *et al.*, 2000).

Alternatively, a Clark-type electrode should be used to measure the production of hydrogen, because this method can measure hydrogen production directly, and this method can also measure hydrogen in the solution phase.

In this experiment, the production of hydrogen was inferred by observing the reduction of BV by the SH as a result of electron flow from the oxidation of methanol by BmMDH S97G.

Chapter 7: Conclusions

This thesis examined the following: (1) the effects of amino acid substitution on the enzymatic properties and purification of the methanol dehydrogenase from *B. methanolicus* C1; (2) the expression, purification, and activity of the soluble hydrogenase from *W. eutropha H16* cultured under aerobic conditions; (3) and the identification of electron flow during coupled enzyme reactions. The most important findings in each one are summarized.

The serine to glycine amino acid substitution in Motif A at position 97 of *B. methanolicus* C1 of the MDH protein was successfully demonstrated, resulting in a recombinant BmMDH that can oxidize methanol without the presence of the activator protein.

The protein purification strategies used for isolating BmMDH were also successful. The heat denaturing procedure used to isolate the BmMDH resulted in a high fold purification and high recovery of the protein within a single protein extraction step. In addition, the batch protein purification using affinity dye resin proved to be an efficient method of isolating BmMDH in a single chromatography step. However, the BmMDH activity was lost after purification by the affinity dye resin.

Culturing of *W. eutropha* H16 under aerobic conditions in minimal mineral salt media supplemented was successful. This culturing procedure also resulted in the expression of the soluble hydrogenase that displayed H_2 oxidation activity after being partially purified under aerobic conditions. The protein purification strategy used increased the SH specific activity toward H_2 oxidation. However, the protein

purification strategy did not result in isolation of the SH. In addition, the SH activity was lost after purification by the affinity dye resin.

The coupled enzyme reaction using the NAD-dependent enzymes of methanol dehydrogenase from *Bacillus methanolicus* and the hydrogenase from *W. eutropha* in the presence of methanol resulted in the reduction of benzyl viologen, thus demonstrating the generation of electron flow and inferring the production of hydrogen.

Bibliography

Adams, M. W. W., Mortenson, L. E. and Chen, J.-S. (1981). Hydrogenase. *Biochimica et Biophysica Acta* **594**:105-176.

Alves, A. M. C. R., Euverink, G. J. W., Hektor, H. J., Hessels, G. I., Van der Vlag, J., Vrijbloed, J. W., Hondmann, D., Visser, J., and Dijkhuizen, L.. (1994). Enzymes of glucose and methanol metabolism in the actinomycete *Amycolatopsis methanolica*. *J. Bacteriol* **176**:6827-6835.

Ananthachar, V., and Duffy, J. J. (2005). Efficiencies of hydrogen storage systems onboard fuel cell vehicles. *Solar Energy* **78**: 687-694.

Anthony, C. (1986). Bacterial oxidation of methane and methanol. *Advanced Microbiology and Physiology* **27**: 113-210.

Arfman, N., Hektor, H. J., Bystrykh, L. V., Govorukhina, N. I., Dikhuizen, L., and Frank, J. (1997). Properties of an NAD(H)-containing methanol dehydrogenase and its activator protein form *Bacillus methanolicus*. *European Journal of Biochemistry* **244**: 426-433.

Arfman, N., Watling, E. M., Clement, W., van Oosterwijk, R. J., De Vries, G. E., Harder, W., Attwood, M. M., and Dijkhuizen, L. (1989). Methanol metabolism in thermotolerant methylotrophic *Bacillus* strains involving a novel catabolic NAD-dependent methanol dehydrogenase as a key enzyme. *Archives of Microbiology* **152**: 280-288.

Arfman, N., Van Beeumen, J., De Vries, G. E., Harder, W., and Dijkhuizen, L. (1991). Purification and characterization of an activator protein for methanol dehydrogenase from thermotolerant *Bacillus spp*. *Journal of Biological Chemistry* **266**: 3955-3960.

Arfman, N., De Vries, K. J., Moezelaar, H. R., Attwood, M. M., Robinson, G. K., van Geel, M., and Dijkhuizen, L. (1992). Environmental regulation of alcohol metabolism in thermotolerant methylotrophic *Bacillus* strains. *Archives of Microbiology* **157**: 272-278.

Bernhard, M., Schwartz, E., Rietdorf, J., and Friedrich, B. (1996). The *Alcaligenes eutrophus* membrane-bound hydrogenase gene locus encodes functions

involved in maturation and electron transport coupling. *Journal of Bacteriology* **178**: 4522-5429.

Bernhard, M., Buhrke, T., Bleijlevens, B., De Lacey, A. L., Fernandez, V. M., Albracht, S. P., and Friedrich, B. (2001). The H_2 sensor of *Ralstonia eutropha*: Biochemical characteristics, spectroscopic properties, and its interaction with a histidine protein kinase. *Journal of Biological Chemistry* **276**: 15592-15597.

Bessman, M. J., Frick, D. N., and O'Handley, S.F. (1996). The MutT proteins or "nudix" hydrolases, a family of versatile, widely distributed, "housecleaning" enzymes. *Journal of Biological Chemistry* **271**: 25059-25062.

Bitsche, O., and Gutmann, G. (2004). Systems for hybrid cars. *Journal of Power Sources* **127**: 8-15.

Bleijlevens, B., Buhrke, T., Van der Linden, E., Friedrich, B., and Albracht, S. P. J. (2004). The auxiliary protein HypX provides oxygen tolerance to the soluble [NiFe]-hydrogenase of *Ralstonia eutropha* H16 by way of a cyanide ligand to nickel. *Journal of Biological Chemistry* **279**: 46686-46691.

Blokesch, M., Albracht, S. P., Matzanke, B. F., Drapal, N. M., Jacobi, A., and Bock, A. (2004). The complex between hydrogenase-maturation proteins HypC and HypD is an intermediate in the supply of cyanide to the active site iron of [NiFe]-hydrogenases. *Journal of Molecular Biology* **344**: 155-167.

Boettner, D. D. and Moran, M. J. (2004). Proton exchange membrane (PEM) fuel cell-powered vehicle performance using direct-hydrogen fuelling and on-board methanol reforming. *Energy* **29**: 2317-2330.

Buhrke, T., Bleijlevens, B., Albracht, S. P., and Friedrich, B. (2001). Involvement of hyp gene products in maturation of the H(2)-sensing [NiFe] hydrogenase of Ralstonia eutropha. *Journal of Bacteriology* **183**:7087-7093.

Burgdorf, T., Loscher, S., Liebisch, P., Van der Linden, E., Galander, M., Lendzain, F., Meyer-Klaucke, W., Albracht, S. P. J., Friedrich, B., Dau, H. and Haumann, M. (2005). Structural and oxidation-state changes at its non-standard Ni-Fe site during activation of the NAD-reducing hydrogenase form *Ralstonia eutropha* detected by X-ray absorption, EPR, and FTIR spectroscopy. *Journal of American Chemical Society* **127**: 576-592.

Burton, S. G. (2001). Development of bioreactors for application of biocatalysts in biotransformations and bioremediation. *Pure Applied Chemistry* **73**: 77–83.

Bystrykh, L. V., Vonck, J., Van Bruggen, E. F. J., Van Beeumen, J., Samyn, B., Govorukhina, N. I., Arfman, N., Duine, J. A., and Dijkhuizen, L. (1993a). Electron microscopic analysis and structural characterization of novel NADP(H)-containing methanol:N,N'-dimethyl-4-nitrosoaniline oxidoreductases from the Gram-positive methylotrophic bacteria *Amycolatopsis methanolica* and *Mycobacterium gastri* MB19. *Journal of Bacteriology* **175**:1814-1822.

Cammack, R., Frey, M., and Robson, R. (2001). *Hydrogen as a fuel: Learning from nature*. Taylor & Francis, London.

Cammack, R., Fernandez, V. M., and Hatchikian, E. C. (1994). Nickel-iron hydrogenase. *Methods in Enzymology* **243**: 43-68.

Casalot, L., and Rousset, M. (2001). Maturation of the [NiFe] hydrogenases. *Trends in Microbiology* **9**: 228-237.

Chmielniak, T., and Sciazko, M. (2003). Co-gasification of biomass and coal for methanol synthesis. *Applied Energy* **74**: 393-403.

Clauss, R., Mayes, J., Hilton, P., and Lawrenson, R. (2005). The influence of weather and environment on pulmonary embolism: pollutants and fossil fuels. *Medical Hypotheses* **64**: 1198-1201.

Das, D., and Veziroglu, T. N. (2001). Hydrogen production by biological processes: A survey of literature. *International Journal of Hydrogen Energy* **26**: 13-28.

Davis, D. L. (1997). Short-term improvements in public health from global-climate policies on fossil-fuel combustion: An interim report. *The Lancet* **350**: 1341-1349.

De Hoop, M. J., S. Asgeirsdottir, M. Blaauw, M. Veenhuis, J. Cregg, M. Gleeson, and G. AB. (1991). Mutations in the FAD-binding fold of alcohol oxidase from *Hansenula polymorpha*. *Protein Engineering* **4**: 821-829.

Dernedde J, Eitinger T, Patenge N., and Friedrich, B. (1996). Hyp gene products in *Alcaligenes eutrophus* are part of a hydrogenase-maturation system. *European Journal of Biochemistry* **235**: 351-358.

De Vries, G. E., Arfamn, N., Terpstra, P., and Dijkhuizen, L. (1992). Cloning, expression, and sequence analysis of the *Bacillus methanolicus* C1 methanol dehydrogenase gene. *Journal of Bacteriology* **174**: 5346-5353.

Dieffenbach, C. W., and Dveksler, G. S. (2003). *PCR primer: A laboratory manual*, 2nd ed. Cold Spring Harbor Laboratory Press, New York.

Dijkhuizen, L., Arfman, N., Attwood, M. M., Brooke, A. G., Harder, W., and Watling, E. M. (1988). Isolation and initial characterization of thermotolerant methylotrophic *Bacillus* strains. *FEMS Microbiology Letters* **52**: 209-214.

Dixon, M., and Webb, E. C. (1965). *Enzymes*, Second ed. Longmans, Green and Company, London.

Fontecilla-Camps, J. C., Frey, M., Garcin, E., Hatchikian, C., Montet, Y., Piras, C., Vernede, X., and Volbeda, A. (1997). Hydrogenase: A hydrogen-metabolizing enzyme. What do the crystal structures tell us about its mode of action? *Biochimie* **79**: 661-666.

Friedrich, B., Buhrke, T., Burgdorf, T., and Lenz O. (2005). A hydrogen-sensing multiprotein complex controls aerobic hydrogen metabolism in *Ralstonia eutropha*. *Biochemical Society Transactions* **33**: 97-101.

Graf, E.–G., and Thauer, R. K. (1981). Hydrogenase form *Methanobacterium thermoautotrophicum*, a nickel-containing enzyme. *FEMS Microbiology Letters* **136**: 165-169.

Harder, W., and Veehuis, M. (1989). "Metabolism of one-carbon compounds." In: *The yeasts* (Rose, A.H. and Harrison, J.S. Eds) Second ed., Vol. 3: 289-316. Academic Press, London.

Hektor, H. J., Kloosterman, H., and Dijkhuizen, L. (2002). Identification of a magnesium-dependent NAD(P)(H)-binding domain in the nicotinoprotein methanol dehydrogenase from *Bacillus methanolicus*. *Journal of Biological Chemistry* **277**: 46966-46973.

Huang H. Q., Lin Q. M., Zhai W. J., and Chen, C. H. (2000). Effect of redox mediators on nitrogenase and hydrogenase activities in Azotobacter vinelandii. *Journal of Protein Chemistry* **19**: 671-678.

Islam, M., Fartaj, A., and Ting, D. S.-K. (2004). Current utilization and future prospects of emerging renewable energy applications in Canada. *Renewable and Sustainable Energy Reviews* **8**: 493-519.

Johnston, B., Mayo, M. C., and Khare, A. (2005). Hydrogen: The energy source for the 21st century. *Technovation* **25**: 569-585.

Jones, A. K., Lenz, O., Strack, A., Buhrke, T., and Friedrich, B. (2004). NiFe hydrogenase active site biosynthesis: Identification of Hyp protein complex in *Ralstonia eutropha*. *Biochemistry* **43**: 13467-13477.

Kato, T., Berger, S. J., Carter, J. A., and Lowry, O. H. (1973). An enzymatic cycling method for nicotinamide-adenine dinucleotide with malic and alcohol dehydrogenases. *Analytical Biochemistry* **53**: 86-97.

Kloosterman, H., Vrijbloed, J. W., and Dijkhuizen, L. (2002). Molecular, biochemical, and functional characterization of a Nudix hydrolase protein that stimulates the activity of a nicotinoprotein alcohol dehydrogenase. *Journal of Biological Chemistry* **277**(38): 34785-34792.

Kortluke, C., and Friedrich, B. (1992). Maturation of membrane-bound hydrogenase of *Alcaligenes eutrophus* H16. *Journal of Bacteriology* **174**: 6290-6293.

Kroutil, W., Mang, H., Edegger, K., and Faber, K. (2004). Recent advances in the biocatalytic reduction of ketones and oxidation of *sec*-alcohols. *Current Opinion in Chemical Biology* **8**: 120-126.

Lapuerta, M., Armas, O., Ballesteros, R., and Fernández, J. (2005). Diesel emissions from biofuels derived from Spanish potential vegetable oils. *Fuel* **84**: 773-780.

Lenz, O., and Friedrich, B. (1998). "A novel multicomponent regulatory system mediates H_2 sensing," in *Alcaligenes eutrophus. Proceedings of the National Academy of Sciences* **95**: 12474-12479.

Lesk, A. M. (1995). NAD-binding domains of dehydrogenases. *Current Opinions in Structural Biology* **5**:775-783.

Levin, D. B., Pitt, L., and Love, M. (2004). Biohydrogen production: Prospects and limitations to practical application. *International Journal of Hydrogen Energy* **29**: 173-185.

Van der Linden, E., Burgdorf, T., Bernhard, M., Bleijlevens, B., Friedrich, B., and Albracht, S. P. J. (2004a). The soluble [NiFe]-hydrogenase from *Ralstonia eutropha* contains four cyanides in its active site, one of which is responsible for the insensitivity towards oxygen. *Journal of Biological and Inorganic Chemistry* **9**: 616-626.

Van der Linden, E., Faber, B. W., Bleijlevens, B., Burgdorf, T., Bernhard, M., Friedrich, B., and Albracht, S. P. J. (2004b). Selective release and function of one of two FMN groups in the cytoplasmic NAD^+-reducing [NiFe]-hydrogenase from *Ralstonia eutropha. European Journal of Biochemistry* **271**: 801-808.

Littlechild, J. A., Guy, J. E. and Isupov, M. N. (2004). Hyperthermophilic dehydrogenase enzymes. *Biochemical Society Transactions* **32**: 255-258.

Loscher, S., Burgdorf, T., Buhrke, T., Friedrich, B., Dau, H., and Haumann, M. (2005). Non-standard structures of the Ni-Fe cofactor in the regulatory and the NAD-reducing hydrogenases from Ralstonia eutropha. Biochem Soc Trans. **33**: 25-27.

Maier, T., Lottspeich, F., and Bock, A. (1995). GTP hydrolysis by HypB is essential for nickel insertion into hydrogenases of *Escherichia coli. European Journal of Biochemistry* **230**: 133-138.

Massanz, C., Fernandez, V. M., and Friedrich, B. (1997). C-terminal extension of the H_2-activating subunit, HoxH, directs maturation of the NAD reducing hydrogenase in *Alcaligenes eutrophus. European Journal of Biochemistry* **245**: 441-448.

Massanz, C., Schmidt, S., and Friedrich, B. (1998). Subforms and in vitro reconstitution of the NAD-reducing hydrogenase of *Alcaligenes eutrophus. Journal of Bacteriology* **180**: 1023-1029.

Momirlan, M., and Veziroglu, T. N. (2005). The properties of hydrogen as fuel tomorrow in sustainable energy system for a cleaner planet. *International Journal of Hydrogen Energy* **30**: 795-802.

Montet, Y., Amara, P., Volbeda, A., Vernede, X., Hatchikian, E. C., Field, M. J., Frey, M., and Fontecilla-Camps, J. C. (1997). Gas access to the active site of Ni-Fe hydrogenase probed by X-ray crystallography and molecular dynamics. *Nature Structural Biology* **4**: 523-526.

Muller, M. (1993). The hydrogenosome. *Journal of General Microbiology* **139**: 2879-2889.

Nandi, R., and Sengupta, S. (1998). Microbial production of hydrogen: An overview. *Critical Reviews in Microbiology* **24**: 61-84.

Nunez A., Foglia T. A., and Piazza G. J., (1999). Cofactor recycling in a coupled enzyme oxidation-reduction reaction: Conversion of omega-oxo-fatty acids into omega-hydroxy and dicarboxylic acids. *Biotechnology and Applied Biochemistry* **29**: 207-212.

Olsen, J. W., Methta, N. S., and Maier, R. J. (2001). Requirement of nickel metabolism proteins HypA and HypB for full activity of both hydrogenase and urease in *Heliobacter pylori. Molecular Microbiology* **39**: 176-182.

Page, C. C., Moser, C. C., Chen, X., and Dutton, P. L. (1999). Natural engineering principles of electron tunnelling in biological oxidation-reduction. *Nature* **402**: 47-52.

Paschos, A., Bauer, A., Zimmermann, A., Zehelein, E., and Bock, A. (2002). HypF, a carbamoyl phosphate-converting enzyme involved in [NiFe] hydrogenase maturation. *Journal of Biological Chemistry* **277**: 49945-49951.

Peppley, B. A., Amphlett, J. C., Kearns, L. M., and Mann, R. F. (1999). Methanol–steam reforming on $Cu/ZnO/Al_2O_3$ catalysts. Part 2. A comprehensive kinetic model. *Applied Catalysis A: General* **179**: 31-49.

Potoglou, D., and Kanaroglou, P. S. (2005). Carbon monoxide emissions from passenger vehicles: predictive mapping with an application to Hamilton, Canada. *Transportation Research Part D: Transport and Environment* **10**: 97-100.

Price, N. C., and Stevens, L. (1989). *Fundamentals of enzymology*, Second ed. Oxford Science Publication, Oxford.

Reid, M. F., and Fewson, C. A. (1994). Molecular characterization of microbial alcohol dehydrogenases. *Critical Review in Microbiology* **20**: 13-56.

Reismann, S., Hochleitner, E., Wang, H., Paschos, A., Lottspeich, F., Glass, R. S., and Bock, A. (2003). Taming of a poison: Biosynthesis of the NiFe-hydrogenase cyanide ligands. *Science* **229**: 1067-1070.

Sambrook, J., Fritsch, E. F., and Maniatis, T. (1989). Molecular cloning: *A laboratory manual*, Second ed. Cold Spring Harbor Laboratory Press, New York.

Schlegel, H. G., Kaltwasser, H., and Gottschalk G. (1961). Ein Submersverfahren zur Kultur wasserstoffoxydierender Bakterien: Wachstumsphsiologische Untersuchugen. *Archiv fur Mikrobiologie* **38**: 209-222.

Schneider, K., Pinkwart, M., and Jochim, K. (1983). Purification of hydrogenases by affinity chromatography on Procion Red-agarose. *Journal of Biochemistry* **213**: 391-398.

Schneider, K., and Schlegel, H.G. (1976). Purification and properties of soluble hydrogenase from *Alcaligenes eutrophus* H16. *Biochimica et Biophysica Acta* **452**: 66-80.

Schwartz, E., Buhrke, T., Gerischer, U., and Friedrich, B. (1999). Positive transcriptional feedback controls hydrogenase expression in *Alcaligenes eutrophus* H16. *Journal of Bacteriology* **181**: 5684-5692.

Schwartz, E., Gerischer, U., and Friedrich, B. (1998). Transcriptional regulation of *Alcaligenes eutrophus* hydrogenase genes. *Journal of Bacteriology* **180**: 3197-3204.

Schwartz, E., Henne, A., Cramm, R., Eitinger, T., Friedrch, B., and Gottschalk, G. (2003). Complete nucleotide sequence of pHG1: A *Ralstonia eutropha* H16 megaplasmid encoding key enzymes of H_2-based lithoautography and anaerobiosis. *Journal of Molecular Biology* **332**: 369-383.

Thiemermann, S., Dernedde, J., Bernhard, M., Schroeder, W., Massanz, C., and Friedrich, B. (1996). Carboxy-terminal processing of the cytoplasmic NAD-reducing hydrogenase of *Alcaligenes eutrophus* requires the *hoxW* gene product. *Journal of Bacteriology* **178**: 2368-2374.

Tissot, B. (2001). Quel avenir pour les combustibles fossiles? Les avancées scientifiques et technologiques permettront-elles la poursuite d'un développement soutenable avec les énergies carbonées?: What a future for fossil fuels? Will scientific and technological progresses warrant growth of use in carbon-based fuels? *Comptes Rendus de l'Académie des Sciences - Series IIA - Earth and Planetary Science* **333**: 787-796.

Tran-Betcke, A., Warnecke, U., Bocker, C., Zaborosch, C., and Friedrich, B. (1990). Cloning and nucleotide sequences of the genes for the subunits of NAD-reducing hydrogenase of *Alcaligenes eutrophus* H16. *Journal of Bacteriology* **172**: 2920-2929.

Verhagen, M.F., O'Rourke, T., and Adams, M.W. (1999). The hyperthermophilic bacterium, *Thermotoga maritima*, contains an unusually complex iron-hydrogenase: amino acid sequence analyses versus biochemical characterization. *Biochimica et Biophysica Acta* **1412**: 212-229.

Vignais, P.M., Colbeau, A., Willson, J.C. and Jouanneau, Y. (1985). Hydrogenase, nitrogenase and the hydrogen metabolism in photosynthetic bacteria. *Biochimie* **60**: 245-260.

Vignais, P. M., Billoud, B., and Meyer, J. (2001). Classification and phylogeny of hydrogenases. *FEMS Microbiology Reviews* **25**: 455-501.

Volbeda, A., Charon, M.H., de Lacey, A.L., Hatchikian, E.C., and Fontecilla-Camps, J.C. (1995). Crystal structure of the nickel-iron hydrogenase from *Desolfovibrio gigas. Nature* **373**: 580-587.

Vonck, J., Arfman, N., De Vries, G. E., Van Beeumen, J., Van Bruggen, E. F., and Dijkhuizen L. (1991). Electron microscope analysis and biochemical characterization of a novel methanol dehydrogenase from the thermotolerant *Bacillus sp.* C1. *Journal of Biological Chemistry* **266:** 3949-3954.

Wierenga, R. K. and J. Drenth. (1983). Comparison of the three-dimensional protein and nucleotide structure of the FAD-binding domain of *p*-hydroxybenzoate hydroxylase with the FAD- as well as NADPH-binding domains of glutathione reductase. *Journal of Molecular Biology* **167**: 725-739.

Woodward, J., Orr, M., Cordray, K., and Greenbaum, E. (2000). Enzymatic production of biohydrogen. *Nature* **405**: 1014-1015.

Woese, C.R. (1994). There must be prokaryote somewhere. Microbiology's search for itself. *Microbiol. Rev.* **58**: 1-9.

Wuebbles, D. J., and Jain, A. K. (2001). Concerns about climate change and the role of fossil fuel use. *Fuel Processing Technology* **71**: 99-119.